HHS Public Access

Author manuscript

Cell Rep. Author manuscript; available in PMC 2021 September 13.

Published in final edited form as:

Cell Rep. 2021 August 10; 36(6): 109525. doi:10.1016/j.celrep.2021.109525.

Integration of T helper and BCR signals governs enhanced plasma cell differentiation of memory B cells by regulation of CD45 phosphatase activity

Peter Szodoray[1,2,6,*], **Tor Kristian Andersen**[1,3], **Julia Heinzelbecker**[1,2], **John F. Imbery**[1,2], **Peter C. Huszthy**[1], **Stephanie M. Stanford**[4], **Bjarne Bogen**[1,3], **Ole B. Landsverk**[5], **Nunzio Bottini**[4], **Anders Tveita**[1,2], **Ludvig A. Munthe**[1,2], **Britt Nakken**[1,2]

[1]Department of Immunology, University of Oslo and Oslo University Hospital-Rikshospitalet, 0372 Oslo, Norway

[2]K.G. Jebsen Center for B Cell Malignancies, Institute of Clinical Medicine, Faculty of Medicine, University of Oslo, Oslo, Norway

[3]K.G. Jebsen Center for Influenza Vaccine Research, Institute of Clinical Medicine, Faculty of Medicine, University of Oslo, Oslo, Norway

[4]Division of Rheumatology, Allergy and Immunology, Department of Medicine, University of California, San Diego, 9500 Gilman Drive MC #0656, La Jolla, CA 92093, USA

[5]Department of Pathology, University of Oslo and Oslo University Hospital-Rikshospitalet, 0372 Oslo, Norway

[6]Lead contact

SUMMARY

Humoral immunity relies on the efficient differentiation of memory B cells (MBCs) into antibody-secreting cells (ASCs). T helper (Th) signals upregulate B cell receptor (BCR) signaling by potentiating Src family kinases through increasing CD45 phosphatase activity (CD45 PA).

In this study, we show that high CD45 PA in MBCs enhances BCR signaling and is essential for their effective ASC differentiation. Mechanistically, Th signals upregulate CD45 PA through intensifying the surface binding of a CD45 ligand, Galectin-1. CD45 PA works as a sensor of T cell help and defines high-affinity germinal center (GC) plasma cell (PC) precursors characterized by IRF4 expression *in vivo*. Increasing T cell help *in vitro* results in an incremental

*Correspondence: peter.szodoray@medisin.uio.no.

AUTHOR CONTRIBUTIONS

B.N. and P.S. planned and executed experiments, analyzed data, and wrote the manuscript. S.M.S. and N.B. developed and provided the pCAP-SP1 peptide and interpreted data. B.N., P.S., T.K.A., P.C.H., J.H., J.F.I., A.T., and O.B.L. performed experiments. B.B., A.T., and L.A.M. contributed murine models for influenza vaccination, provided protocols, and interpreted data. All authors reviewed the manuscript and provided scientific input.

SUPPLEMENTAL INFORMATION

Supplemental information can be found online at https://doi.org/10.1016/j.celrep.2021.109525.

DECLARATION OF INTERESTS

The authors declare no competing interests.

CD45 PA increase and enhances ASC differentiation by facilitating effective induction of the transcription factors IRF4 and BLIMP1. This study connects Th signals with BCR signaling through Galectin-1-dependent regulation of CD45 PA and provides a mechanism for efficient ASC differentiation of MBCs.

Graphical abstract

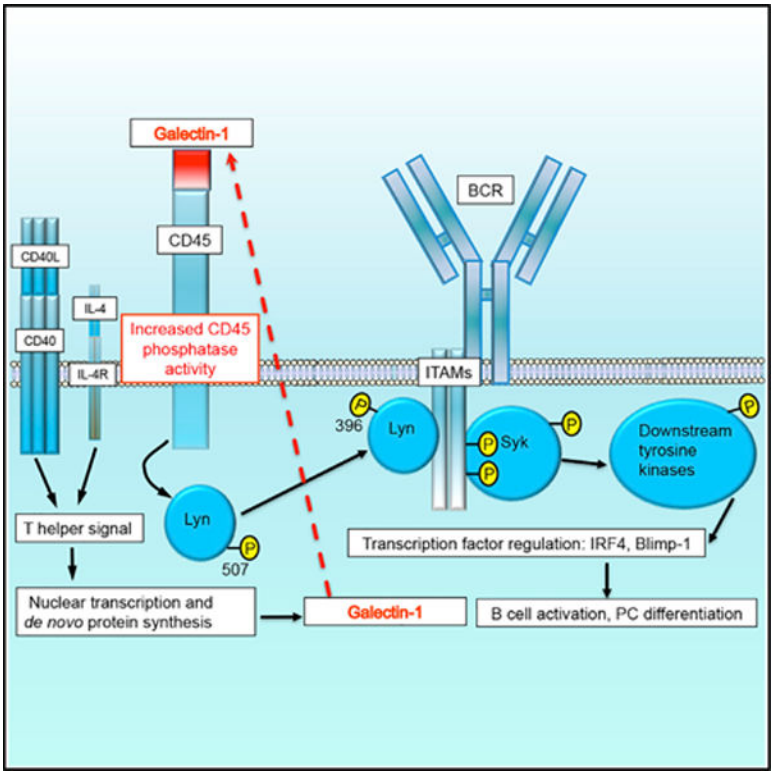

In brief

Szodoray et al. demonstrate that T helper signals upregulate CD45 phosphatase activity in B cells through increased binding of Galectin-1 to CD45. High CD45 phosphatase activity in memory B cells controls their effective differentiation toward antibody-secreting cells in response to T cell help.

INTRODUCTION

Immunological memory is the ability to respond with increased efficacy upon re-challenge with antigen (Ag) (Arpin et al., 1997; Tangye and Tarlinton, 2009). Humoral memory consists of anti-body-secreting effector cells (ASCs) and memory B cells (MBCs), with the latter characterized by rapid re-activation upon secondary Ag challenge (Kurosaki et al., 2015). Several features of MBCs contribute to their enhanced ability to respond upon re-exposure to Ag such as increased B cell receptor (BCR) affinity for Ag (Rajewsky, 1996) and class-switch recombination to immunoglobulin G (IgG) contributing to enhanced BCR signaling (Lutz et al., 2015). Also, intrinsic differences in initiation of BCR signaling

such as activation of early signaling kinases is more robust in human MBCs, irrespective of Ig class (Davey and Pierce, 2012). Studies where IgG1 was expressed in naive B cells showed that antigen-experienced $IgG1^+$ MBCs rapidly differentiated into ASCs, while $IgG1^+$ "naive" B cells did not (Kometani et al., 2013), emphasizing stimulation history in MBC recall efficiency.

CD45 is a protein tyrosine phosphatase that enhances Agmediated signaling in B cells by activating members of the Src family kinases (SFKs) (Zikherman et al., 2012). CD45 dephosphorylates an inhibitory phosphorylated tyrosine (pTyr) on SFKs, leading to autophosphorylation of an activating Tyr resulting in full kinase activity (Hermiston et al., 2003). Genetic manipulation of expression levels of CD45 revealed faulty B cell tolerance in CD45 knockout (KO) mice (Cyster et al., 1996), while enhanced CD45 expression resulted in aberrant B cell activation, autoantibody production, and autoimmunity (Hermiston et al., 2005; Zikherman et al., 2012). Taken together, these data emphasize the critical role of CD45 phosphatase activity in regulating B cell signaling.

Glycosylation status of CD45 has been implicated in regulating binding of natural ligands, such as galectins, which can alter the functional properties of CD45 (Cao et al., 2018; Earl et al., 2010; Giovannone et al., 2018; Nguyen et al., 2001). Galectins are a family of lectins with the ability to bind glycans through one or more carbohydrate-recognition domains (CRDs) that exhibit immunomodulatory properties (Sundblad et al., 2017). Galectins are found intracellularly, but they are also secreted through a non-classical secretory mechanism (Popa et al., 2018). The secreted forms are found both in the extracellular space and bound to surface glycoconjugates such as CD45 (Earl et al., 2010; Hughes, 1999). Among galectins, Galectin-1 is implicated in the regulation of both T and B cell function (Sundblad et al., 2017). Although the role of Galectin-1 in the control of the immune responses mediated by T cells is well characterized, less is known about Galectin-1 function in B cells. During B cell maturation, Galectin-1 interacts with the precursor (pre-)BCR and stromal cells in the bone marrow (BM), leading to pre-BCR signaling and differentiation (Bonzi et al., 2015; Elantak et al., 2012; Espeli et al., 2009). Moreover, Galectin-1 expression was found in pre-B cell acute lymphoblastic leukemia (BP-ALL), and Galectin-1 inhibition reduced migration of BP-ALL cells as well as cell cycle progression and was cytostatic for BP-ALL cells (Paz et al., 2018). Galectin-1 may also provide survival advantages of malignant cells of mature phenotype such as chronic lymphocytic lymphoma (CLL) cells, where Galectin-1 expressed by nurse-like cells was found to modulate Ag signaling in CLL cells (Croci et al., 2013). Moreover, Galectin-1 is important for the regulatory function of B cells (Alhabbab et al., 2018). Mice deficient of Galectin-1 ($Gal\text{-}1^{-/-}$) showed loss of interleukin (IL)-10^+ regulatory B cells, exhibited impaired IL-10 secretion, and were less suppressive *in vitro* and *in vivo* (Alhabbab et al., 2018). Collectively, these studies highlight a role for Galectin-1 in B cell signaling and survival mechanisms; however, a link to CD45 phosphatase activity in B cells has yet to be described.

ASCs differentiate following activation of B cells with cognate Ag in combination with signals from T helper (Th) cells (Mesin et al., 2016). Signals from the BCR and T follicular helper (T_{FH}) cells through CD40L-CD40 interaction activate a transcriptional program regulating plasma cell (PC) differentiation while antagonizing the germinal center (GC)

transcriptional program (Nutt et al., 2015). Interferon regulatory factor 4 (IRF4) is one of the key transcription factors involved in fate decisions of activated B cells, and it functions in a dose-dependent manner: low levels promote GC fate through regulation of Bcl6, whereas high levels of IRF4 repress Bcl6 and activate PR domain zinc finger protein 1 (*Prdm1*), encoding BLIMP1, a transcriptional repressor crucial for PC differentiation (Ochiai et al., 2013; Sciammas et al., 2006; Yasuda et al., 2011). Induction of PC transcription factors is triggered by BCR signaling (Sciammas et al., 2011; Yasuda et al., 2011). The extracellular signal-regulated kinase (ERK) signaling pathway is a key signaling mediator of downstream signaling following BCR ligation. It plays an important role in cell proliferation and also in driving the differentiation of B cells toward the ASC fate by inducing the expression of BLIMP1 (Yasuda et al., 2011). Less is known about the integration of signals emanating from the BCR and T cell help in inducing transcription factors that drive PC differentiation.

We reported that Th signals impact BCR signaling by increasing CD45 phosphatase activity (Szodoray et al., 2016). We hypothesized that MBCs may exhibit increased CD45 phosphatase activity due to dependence on Th cells, representing an internal re-wiring process contributing to increased ASC differentiation upon repeated Ag encounters.

We herein demonstrate that MBCs exhibit a robust increase in CD45 phosphatase activity compared to their naive counterparts, resulting in increased BCR signaling capacity, as shown by enhanced activation of the key BCR signaling kinases, Syk and Erk. The highest level of CD45 phosphatase activity was detected in ASCs. The ability to differentiate toward ASCs in response to Th signals was increased in MBCs and showed strict dependence on CD45 phosphatase activity. Mechanistically, the CD45 ligand Galectin-1 acted as a positive regulator of CD45 phosphatase activity in B cells, and Th signals upregulated surface binding of Galectin-1, facilitating efficient PC differentiation.

RESULTS

CD45 phosphatase activity is increased in human MBCs

Humoral memory is highly dependent on Th cells (Berkowska et al., 2011), and this prompted us to investigate CD45 phosphatase activity within MBCs. CD45 phosphatase activity was significantly increased in human peripheral blood $CD19^+$ B cells expressing the memory marker CD27 (Figures 1A and 1B). A significant increase in CD45 surface expression on $CD27^+$ B cells was noted, although by a smaller magnitude than that of CD45 phosphatase activity (Figure 1C). CD45 protein expression levels in $CD27^+$ MBCs was related to CD45 phosphatase activity (Figures 1D). $CD45^{lo}$ MBCs expressed the same level of CD45 as did naive B cells; nevertheless, $CD45^{lo}$ MBCs had significantly increased CD45 activity (Figure 1E and 1F). To investigate individual CD45 isoforms, human peripheral B cells were stained using CD45RA-, RB-, RC-, and RO-specific antibodies, and no evidence of alterations in isoform expression correlating with increased CD45 phosphatase activity was found (Figure S1A). Taken together, mechanisms regulating both CD45 surface expression and mechanisms modulating CD45 phosphatase activity contributed to the net CD45 activity of MBCs.

CD45 phosphatase activity is upregulated upon CD40L stimulation and leads to more potent BCR signaling in MBCs

In search of a mechanism for the increase in CD45 phophatase activity in MBCs, we investigated whether provision of a CD40L signal could upregulate CD45 phosphatase activity. We found that upon CD40L stimulation of MBCs, similar to naive B cells, CD45 phosphatase activity was significantly upregulated compared to control-treated cells (Figures 2A and 2C, upper panel). Moreover, the resultant CD45 activity was significantly increased in CD40L-stimulated MBCs compared to CD40L-treated naive B cells (Figure 2C, upper panel) and required as little as a 1-h incubation with CD40L (Figure 2J). Pan-CD45 surface protein expression did not increase in naive or MBC subsets that received Th signals (Figures 2B and 2C, middle panel) and were corroborated by qRT-PCR analysis of mRNA levels (Figure 2C, lower panel). Taken together, these data show that MBCs preserve the ability to upregulate CD45 phosphatase activity upon receiving Th signals and that the mechanism does not involve increased CD45 surface expression.

In order to determine whether increased CD45 phosphatase activity of MBCs would result in increased BCR signaling, we assayed the activation of Syk and Erk kinases. Both naive and MBCs significantly increased phosphorylation of Syk and Erk kinases upon CD40L ligation (48 h) in a CD45-dependent manner (Figures 2D–2G), while no upregulation of *SYK* or *ERK1* mRNA was evident (Figures 2H and 2I). Furthermore, we observed higher activation of Syk and Erk kinases in MBCs at baseline compared to naive B cells (Figures 2D–2G) corresponding to the elevated CD45 phosphatase activity in MBCs. Next, we investigated BCR signaling capacity of non-class-switched MBCs at baseline and found a distinct increase in $pErk^{+}$ MBCs compared to naive B cells, establishing this enhanced signaling as an intrinsic effect of MBCs (Figure S1B). Moreover, CD40L stimulation in the absence of BCR engagement potentiated both Syk and Erk activation (Figure S1C, middle panel), suggesting that T cell help increased tonic as well as acute BCR signaling. BCR cross-linking alone did not modulate CD45 phosphatase activity itself (Figure S1C, upper panel). We observed co-expression of pCAP-SP1 (CD45 phosphatase activity) with both pSyk and pErk (Figure S1D), reinforcing the mechanistic connection between CD45 phosphatase activity and enhanced BCR signaling. The inclusion of no pCAP-SP1 probe and isotype controls is shown (Figure S1E). In summary, we conclude that the increased CD45 phosphatase activity in human MBCs translated into more potent BCR signaling, with a potential impact on humoral recall responses.

CD45 phosphatase activity is increased in human MBC and antibody-secreting cell subsets

We next combined pCAP-SP1 measurements with multicolor flow cytometry analyses to explore CD45 phosphatase activity within human peripheral B cell subsets. $CD19^{+}$ B cells were subdivided into naive, MBC, and ASC subsets based on the expression of IgM, IgD, CD27, CD38, and CD138 (Figures 3A–3C). We found increased CD45 phosphatase activity in all MBC subsets compared to naive B cells (Figures 3D and 3F). These findings included the atypical DN memory subset, which does not express the classical human memory marker CD27. Similarly, surface expression of CD45 was also increased within MBCs compared to naive B cells, but at a lower magnitude than CD45 activity (Figures 3E and 3G).

To further subdivide the MBC compartment, we utilized the markers CD80 and PD-L2, which in the mouse define a MBC subset with enhanced recall responses and differentiation toward PCs (Zuccarino-Catania et al., 2014). We detected a B cell population co-expressing CD80 and PD-L2 in human peripheral blood that was significantly increased among IgG MBCs (Figure S2A) and exhibited significantly higher CD45 phosphatase activity than did overall IgG MBCs (Figure S2B), suggesting that CD45 activity levels do not segregate entirely with Ig subclass. Analyzing the percentages of CD45 phosphatase activity^{hi} cells within MBC subsets revealed a higher frequency within IgM MBCs than in IgG MBCs (Figure S2C). Having identified PD-L2 and CD80 as markers of high CD45 activity in IgG MBCs, we investigated marker expression within the CD45 activity^{hi} subset of IgM MBCs and detected increased expression of CD95, CXCR3, IRF4, Galectin-1, and CD40 (Figure S2D).

Overall, the highest CD45 activity was noted among the ASCs and plasma blasts ($CD19^{+}CD138^{-}CD27^{hi}CD38^{hi}$, Figure 3C, left panel), and this was further increased within the more mature $CD138^{+}$ ASCs (Figures 3D and 3F). No further increase in CD45 surface expression was observed within the ASC subsets (Figure 3G), suggestive of mechanisms modulating CD45 phosphatase activity in these cells.

We next measured CD45 phosphatase activity in human BM obtained from healthy donors. Long-lived PCs (LLPCs) are reported to reside within the $CD19^{-}CD38^{hi}CD138^{+}$ population, while shorter lived PCs (SLPCs) are detected within the $CD19^{+}$ population (Halliley et al., 2015; Mei et al., 2015). Within the $CD19^{-}$ cells, we detected $CD138^{+}CD38^{+}$ PCs corresponding to the LLPC phenotype, which were $IRF4^{lo}$ (not shown) and intermediate in BLIMP1, in agreement with Halliley et al. (2015) (Figures 3H and 3I). Within the $CD19^{+}$ PCs, a population of $IRF4^{hi}BLIMP1^{hi}$ B cells that were $CD38^{+}$ and $CD138^{+/lo}$ corresponding to the SLPC phenotype was detected (Halliley et al., 2015) (Figure 3H, right panel). We found that LLPCs exhibited a 10-fold increase in CD45 activity compared to mature BM B cells from the same donors, while SLPCs had intermediate CD45 phosphatase activity levels (Figure 3I and 3J). Similar to findings in peripheral ASCs, CD45 phosphatase activity in BM PCs did not correspond to CD45 expression levels (Figures 3I and 3J). Taken together, it appears likely that the increase in CD45 activity in ASCs is explained by a different mechanism than regulation of CD45 surface expression. Overall, the increased CD45 phosphatase activity in MBCs and ASCs may reflect their activation by T cells and could therefore represent an important factor involved in Th-dependent differentiation into ASCs.

Differentiation of antibody-secreting cells by Th signals is CD45-dependent

We next sought to determine whether CD45 was involved in ASC differentiation. Isolated human peripheral B cells from healthy donors were cultured in the presence of Th signals (CD40L, IL-4, IL-21). In all experiments, a viability stain was included to gate out dead cells. As expected, we observed that Th signals drove B cells toward ASC differentiation as defined by expression of CD38 and CD138 (Figure 4A, upper panel). However, when utilizing an inhibitor of CD45 phosphatase activity, the differentiation of ASCs was blocked (Figures 4A and 4B). Intriguingly, when analyzing the expression of the PC marker CD138

versus CD45 phosphatase activity, a clear co-expression could be seen (Figure 4A, lower panel). Upregulation of CD45 phosphatase activity and the ASC-associated markers CD38 and CD138 was observed upon T cell help, and a clear downmodulation was observed upon inhibition of CD45 (Figure 4C, upper panel).

Differentiation of ASCs is a function of BCR signaling and proliferation (Tangye et al., 2003b; Tangye et al., 2002) and is consequently highly dependent on the transcription factors IRF4 and BLIMP1 suppressing the GC and MBC transcriptional programs (Nutt et al., 2015). We noted a CD45-mediated induction of both proliferation (Figure S3A) and expression of BLIMP1 and IRF4 (Figure 4C, lower panel), and, moreover, induction of IRF4 and BLIMP1 expression showed Syk dependence (Figure S3B). Small interfering RNA (siRNA)-mediated silencing of CD45 during a 7-day differentiation of B cells toward ASCs resulted in a significant decrease in ASCs, as evidenced by reduced levels of IRF4 and BLIMP1 double-positive cells (Figures 4D and 4E). Using this strategy, we achieved approximately 30% downregulation in CD45 expression at day 7 post-siRNA delivery with a similar decrease of CD45 phosphatase activity (Figure 4F, upper panel), along with downmodulation of IRF4 and BLIMP1 (Figure 4F, lower panel). Taken together, our data strongly support the involvement of CD45 phosphatase activity in the Th-mediated differentiation of ASCs through instructing the PC-associated transcription factors IRF4 and BLIMP1.

Increasing T cell help leads to an incremental increase in CD45 phosphatase activity and efficient MBC differentiation into ASCs

A defining feature of MBCs is their enhanced ability to differentiate into ASCs during T cell-mediated recall responses (Aiba et al., 2010; Arpin et al., 1997; Hebeis et al., 2004; Moran et al., 2018). The high CD45 phosphatase activity in MBCs, as well as their ability to further upregulate this activity upon T cell help, prompted us to investigate ASC differentiation and its dependence on CD45 phosphatase activity in naive B cells and MBCs. As expected, purified MBCs developed more efficiently into $IRF4^{+}BLIMP1^{+}$ ASCs than did naive B cells, and they showed clear dependence on CD45 (Figures 5A and 5B). Production of IgM and IgG from MBC cultures was significantly increased compared to naive B cell cultures, corroborating the enhanced differentiation of ASCs in MBC cultures (Figure S4A).

Mechanistically, high CD45 phosphatase activity was coexpressed both with BLIMP1 and IRF4 during ASC differentiation (Figure 5E), and MBCs upregulated active Erk kinase (pErk) to higher levels than naive B cells (Figure S4B). Furthermore, pErk and IRF4 were coexpressed in a population of MBCs differentiating toward ASCs, and this pronounced ASC differentiation was blocked by CD45 inhibition (Figure 5F). The $IRF4^{+}BLIMP1^{+}$ ASCs traced back to $pErk^{hi}IRF4^{hi}$ cells (Figure 5G, left and middle panels), and hence this population showed significantly increased expression of pErk compared to overall MBCs (Figures 5G, right panel, and 5H). These data suggest that CD45 activity enhances BCR signaling kinases and ASC differentiation through transcription factors IRF4 and BLIMP1, which is in line with data obtained utilizing an inhibitor to Syk kinase demonstrating involvement of BCR signaling in ASC differentiation (Figure S3B). Provision of BCR cross-linking during cultures did not result in enhanced ASC differentiation (Figures S4D

and S4E). We further noted that treatment with IL-4 and IL-21, alone or in combination, did not lead to upregulation of CD45 phosphatase activity or differentiation of ASCs (Figures S5A and S5B). However, stimulation with CD40L alone was sufficient for upregulation of CD45 phosphatase activity (Figure S5A) but did not lead to ASC differentiation (Figure S5B). Therefore, CD45 phosphatase activity was necessary but not sufficient for driving Th-mediated ASC differentiation.

According to current models, T cell help is the limiting factor both for affinity maturation of GC B cells and selection into the PC fate (Allen et al., 2007; Victora et al., 2010). Thus, to model more effective Th *in vitro*, increasing concentrations of CD40L were provided to stimulate ASC differentiation. We found that ASC differentiation and CD45 phosphatase activity increased with higher doses of CD40L both in naive B cells and MBCs (Figures 5A–5D). Importantly, CD45 phosphatase activity and ASC differentiation were significantly augmented in MBCs compared to naive B cell cultures at all concentrations of CD40L provided (Figures 5A–5D). We furthermore observed an incremental increase in IRF4 expression in both naive and MBCs upon increasing levels of CD40L stimulation. However, MBCs but not naive B cells, reached high levels of IRF4 expression, which were linked to elevated BLIMP1 expression (Figures S5C and S5D). Additionally, MBCs expressing low levels of IRF4 ($IRF4^{lo}$) revealed increased CD45 activity and pErk compared to naive B cells with similar low IRF4 expression (Figure S5E), indicative of CD45- and Erk-mediated transition of $IRF4^{lo}$ to $IRF4^{hi}$ expression in MBCs. Significantly higher $IRF4^{+}BLIMP1^{+}$ B cells and concomitant CD45 activity were detected when isolated PD-$L2^{+}$-compared to PD-$L2^{-}$-switched MBCs were differentiated toward ASCs (Figure S4C). These data are in line with the notion that recall ability is associated with CD45 activity.

In summary, these findings suggest that the mechanism underlying the enhanced differentiation of ASCs from MBCs in the presence of Th factors is mediated by elevated CD45 phosphatase activity. This is linked to enhanced BCR signaling and induction of pivotal transcription factors necessary for the PC transcriptional program.

CD45 phosphatase activity defines high-affinity GC PC precursors in a T cell-dependent vaccination system

Given the findings that incremental amounts of T cell help (CD40L) gave rise to a progressive increase in CD45 phosphatase activity and resultant ASCs, we next investigated CD45 activity in high-affinity GC B cells that are destined for PC selection (Ise et al., 2018; Paus et al., 2006; Phan et al., 2006). BCRs with high affinity for Ag bind and take up Ag more efficiently and present it on major histocompatibility complex (MHC) class II molecules, which in turn will lead to stronger T-B cell interaction through CD40L-CD40, resulting in PC selection (Victora et al., 2010). After verifying that the CD45 phosphatase assay (pCAP-SP1) works in murine B cells (Figure S6A), we utilized a murine influenza vaccination model that effectively generates LLPCs in a T cell-dependent manner (Andersen et al., 2017; Grodeland et al., 2013). Four weeks after immunization, murine lymph node (LN) and BM cell suspensions were analyzed by flow cytometry and gated on GC cells ($B220^{+}GL7^{hi}CD38^{lo}$) (Figure 6A) or PCs ($Blimp1^{+}CD138^{+}$) (Figure 6D). At this time point hemagglutinin (HA)-reactive GC B cells could be detected in draining LNs (Figure S6B, left

panel), anti-HA-secreting cells were found in BM (Andersen et al., 2019), and immunized mice show sero-conversion toward HA (Figure S6B, right panel). No reactivity toward HA was detected in naive mice or in OVA-immunized mice, as evidenced by HA staining (Figure 6A; Figure S6B). A report showed that high-affinity GC B cells destined for PC selection expressed the transcription factor IRF4 (Ise et al., 2018). High-affinity $HA^{+}IgG1^{+}$ GC B cells expressing IRF4 were readily detected (Figures 6A and 6B, right panel) and were found to harbor significantly higher CD45 phosphatase activity compared to low-affinity GC B cells (Figures 6B and 6G). Phenotypically, high-affinity HA-binding GC cells were negative for the PC markers Blimp1, and CD138 (Figure 6C), further confirming their PC precursor identity. In direct parallel to human PCs, murine BM PCs exhibited the highest levels of CD45 phosphatase activity (Figures 6C, left panel, and 6H), which correlated with Blimp1 and IRF4 expression (Figure 6E). Moreover, murine IgG^{+} MBCs harbored intermediate CD45 activity compared to naive B cells and PCs and displayed HA-binding (Figures S6C and S6D). BM PCs displayed strong reactivity toward HA and exhibited the highest HA binding when normalized to IgG (Figures 6F and 6I). Lastly, differentiating murine B cells toward ASCs *in vitro* showed a similar CD45 dependence as previously shown for human B cells (Figure S6E).

In summary, these results demonstrate an incremental increase in CD45 phosphatase activity moving from low- and high-affinity GC cells to BM PCs differentiated in a T cell-dependent manner in the context of an *in vivo* vaccination system. Furthermore, CD45 phosphatase activity defined high-affinity GC PC precursors and connected CD45 phosphatase activity with graded T cell help and BCR affinity for antigen.

Galectin-1 enhances CD45 phosphatase activity and PC-differentiation

In search of a mechanism regulating CD45 phosphatase activity, we investigated the expression of Galectin-1, a lectin recognizing *N*-acetyllactosamine (LacNac) units on branches of *N*- or *O*-linked glycans on cell surface receptors, including CD45 (Fouillit et al., 2000; Nguyen et al., 2001). A stepwise increase in Galectin-1 surface expression for each maturation step was noted for human peripheral blood naive B cells, MBCs, and PCs (Figure 7A, left and middle panels). There was a strong association between Galectin-1 and CD45 phosphatase activity levels, and, furthermore, PCs ($CD138^{hi}CD38^{hi}$) were identical to the Galectin-1^{hi}CD45 $activity^{hi}$ B cells (Figure 7A, right panel). Galectin-1 binding is inhibited by sialic acid modification of Lac-Nac (Amano et al., 2003) and can be enzymatically removed by neuraminidase (NA). NA treatment of human B cells revealed a dose-dependent increase in CD45 phosphatase activity, and a corresponding increase in Galectin-1 surface staining on human peripheral blood B cells (Figure 7B). Reduced staining using the antibody MEM-55 recognizing a sialidated epitope on CD45 (Koethe et al., 2011) confirmed effective sialic acid removal upon NA treatment (Figure 7B). These dramatic responses underscored the effect of Galectin-1 on regulating CD45 phosphatase activity.

We next utilized an inhibitor to Galectin-1, OTX008, a calixarene derivative designed to bind the Galectin-1 amphipathic β sheet conformation (Astorgues-Xerri et al., 2014; Dings et al., 2012). Treatment with OTX008 during *in vitro* culture resulted in a dose-dependent inhibition of differentiation into $IRF4^{+}BLIMP1^{+}$ ASCs (Figure 7C, upper panels).

Analogous to CD45 inhibition, OTX008 also inhibited CD40L-mediated proliferation (Figure S7A). Staining for surface Galectin-1 confirmed downregulation of expression by OTX008 and a concomitant reduction in CD45 phosphatase activity (Figure 7C, lower panels). During ASC differentiation, we observed CD40L-mediated upregulation of surface Galectin-1 as well as CD45 phosphatase activity, both of which were inhibited by OTX008 (Figure S7B). The gated Galectin-1^{hi}CD45 activity^{hi} population was CD138^{+}, confirming a PC precursor identity (Figure S7C). Similarly to CD45 inhibition, OTX008 downregulated the differentiation of pErk^{+}IRF4^{+} ASCs (Figure S7D). Conversely, adding recombinant human (rh) Galectin-1 protein to B cell cultures increased CD45 phosphatase activity in Galectin-1-binding B cells (Figure 7D). We next investigated total Galectin-1 expression (surface + intracellular) levels, and found CD40L-mediated upregulation of Galectin-1 expression, with corresponding increases in Galectin-1 mRNA (*LGALS1*) by qRT-PCR (Figure S7E). Taken together, these data are suggestive of CD40L-mediated autocrine production of the CD45 ligand Galectin-1.

Surveying human TLR ligands revealed a similar upregulation of CD45 activity for CpG as previously found for CD40L (Figure S8A). Further analysis revealed that the CpG-mediated upregulation of CD45 activity led to increased BCR signaling (pSyk) and that this was both CD45- and TLR-dependent (Figure S8B). Investigating the level of CD45 expression revealed that the CpG-mediated increase in CD45 activity could not be explained only by a CD45 expression increase (Figure S8C). Galectin-1 surface expression was signficantly upregulated during CpG stimulation (Figure S8D, left panels) and both CD45 activity and Galectin-1 was reduced by OTX008 (Figure S8D, right panels), evidence of CpG-mediated CD45 activity regulation by Galectin-1. Lastly, investigating both CpG-induced proliferation (Figure S8E) and ASC differentiation (Figure S8F) in the presence of CD45 inhibitor or OTX008 revealed CD45 and Galectin-1 dependence on these processes analogous to Th-mediated proliferation and ASC differentiation.

We next examined the localization of Galectin-1 relative to pSyk, pCAP-SP1 (CD45 phosphatase activity), and CD45 in purified peripheral human B cells by confocal microscopy and found partial to complete colocalization for all of these factors (Figure 7E). The binding of CD45 to Galectin-1 was further supported by co-immunoprecipitation experiments of CLL cells (Figure 7F). Further analysis of the fraction of Galectin-1 colocalizing with CD45 revealed increased co-localization in MBCs compared to naive B cells upon CD40L stimulation (Figure S7F). Lastly, CRISPR-Cas9-mediated knockout of Galectin-1 (*LGALS1*) in Raji B cells resulted in a dramatic reduction of CD45 phosphatase activity, a near background level that was similar to that found in the corresponding CD45 (*PTPRC* gene) knockout (Figure 7G; Figure S7G). Thus, Galectin-1 expression was necessary for CD45 phosphatase activity.

Taken together, the data demonstrate that Galectin-1 rewires B cells both upon T cell-dependent and -independent signals by regulating CD45 phosphatase activity, controlling BCR signaling and enhancing T cell-dependent ASC differentiation of MBCs.

DISCUSSION

We found that MBCs had increased CD45 phosphatase activity compared to their naive counterparts, resulting in stronger BCR signaling capacity, and we linked this to enhanced differentiation toward ASCs. Mechanistically, we established that Th signals upregulated CD45 phosphatase activity through Galectin-1 serving as an activity-regulating CD45 ligand.

These findings support the notion that there are intrinsic differences in BCR signaling capacity between naive and MBCs. In line with this, early BCR signaling events show that human MBCs, irrespective of Ig subclass, recruit and activate signaling-associated kinases more robustly than do naive B cells (Davey and Pierce, 2012). We herein provide evidence that upregulation of CD45 phosphatase activity upon receipt of Th signals was a pivotal mechanism for the increased BCR signaling and activation of signaling-associated kinases Syk and Erk in MBCs. We furthermore demonstrate that the elevated signaling capacity of MBCs was not only due to the enhanced signaling propensity of the IgG molecule (Lutz et al., 2015), since IgM MBCs also had increased pErk levels compared to naive B cells.

Surveys of MBC populations revealed increased CD45 phosphatase activity irrespective of Ig isotype expression. Studies have addressed the question of whether IgM or IgG MBCs harbor more efficient recall responses, with several reports pointing to the IgG MBCs as the more efficient precursor for effector cell differentiation (Benson et al., 2009; Dogan et al., 2009; Gitlin et al., 2016; Kometani et al., 2013; Pape et al., 2011). In contrast, one study found that increased recall ability segregated with expression of CD80 and PD-L2, rather than unequivocally relating to Ig class (Zuccarino-Catania et al., 2014). When subdividing MBCs based on these markers, we find that the IgG MBCs contain a significant proportion of $CD80^{+}PD\text{-}L2^{+}$ B cells, which, importantly, also demonstrated increased CD45 phosphatase activity compared to the total IgG MBC pool and superior ASC-differentiating capability *in vitro*. These data suggest that upregulated CD45 phosphatase activity does not strictly segregate with Ig subclass and that CD80/PD-L2 expression may define a B cell population in humans with increased BCR signaling and recall ability.

The highest levels of CD45 phosphatase activity were observed within the effector cell subsets, both in peripheral blood and BM-derived PC populations. PCs have undergone high levels of somatic hypermutation, express the highest affinity BCRs, and have received most efficient T cell help (McHeyzer-Williams et al., 2011; Phan et al., 2006; Victora and Nussenzweig, 2012). In addition, the ability of MBCs to further upregulate CD45 phosphatase activity and BCR signaling is suggestive of a role in secondary recall responses. In fact, we found that the ability to differentiate into ASCs upon provision of Th signals showed strong dependence on CD45 when utilizing CD45 inhibitor and siRNA approaches. Mechanistically, high CD45 phosphatase activity was observed in a distinct population of B cells developing into $CD138^{+}$ PCs, and CD45 inhibition abrogated induction of expression of the PC transcription factors IRF4 and BLIMP1. In mice, somatic hypermutation and early ASC formation appeared to be unaffected by the loss of CD45 expression in B cells (Huntington et al., 2006). However, these mice had a reduced GC response and impaired

output of high-affinity PCs (Huntington et al., 2006), pointing to a role for CD45 in later stages of GC maintenance and PC differentiation.

BCR affinity for Ag plays an important role in fate decisions of activated B cells, with higher-affinity BCRs tending to favor PC differentiation (Phan et al., 2006). According to current models, high-affinity BCRs bind and take up Ag more efficiently and present it on MHC class II molecules, which in turn will lead to stronger T-B cell interaction through CD40L-CD40 interaction (Victora and Nussenzweig, 2012). Thus, PC differentiation is likely to require stronger T cell helper signals than those necessary for GC initiation and recycling (Ise et al., 2018). We mimicked a stepwise increase of T cell help by stimulating B cells with increasing amounts of CD40L and observed an associated enhanced propensity of MBCs to differentiate into PCs, again showing strong dependence on CD45. A stepwise increase in CD45 phosphatase activity and subsequent PC differentiation was evident for both naive and MBCs, but CD45 phosphatase activity and frequency of ASCs were significantly increased in MBC cultures at all concentrations of CD40L. This likely reflects their previous enhancement of CD45 phosphatase activity through T cell help, providing them with a competitive advantage over naive B cells.

The transcription factor IRF4 regulates GC and PC fates by instructing different transcriptional networks through graded expression levels and subsequent differential binding of gene regulatory motifs (Klein et al., 2006; Ochiai et al., 2013; Sciammas et al., 2006). We observed a gradual increase in CD45 phosphatase activity both in naive B cells and MBCs upon incremental CD40L stimulation. Critically, MBCs, but not naive B cells, reached higher CD45 phosphatase activity levels and IRF4 expression levels, which enabled them to subsequently induce BLIMP1 expression. Expression of IRF4 is induced upon Ag receptor signaling in B and T cells (Sciammas et al., 2011) and also appears linked to BCR signaling in our study based on the observation that active Erk kinase and IRF4 were coexpressed in a population of MBCs differentiating toward ASCs that was abolished by CD45 inhibition. MBCs expressing low levels of IRF4 had increased CD45 activity and pErk compared to naive B cells with equivalent IRF4 expression levels, further supporting a CD45- and Erk-mediated transition of $IRF4^{lo}$ to $IRF4^{hi}$ expression in MBCs.

Apart from the apparent dependence of T cell help (Victora et al., 2010), the requirement for BCR signaling in GC fate decisions has been debated (Khalil et al., 2012). A study showed that signals provided both by the BCR and by T_{FH} cells are required for PC generation from GC B cells (Kräutler et al., 2017), and transcriptome analysis of PC precursors revealed signatures of both BCR and CD40 activation (Ise et al., 2018). Furthermore, strong CD40 and BCR stimulation led to Cbl degradation and upregulation of IRF4 and GC exit (Li et al., 2018). Previously, it was suggested that both BCR signaling kinases Syk and Erk in concert promote PC differentiation by cancelling PAX5-mediated repression of BLIMP1 (Inagaki et al., 2016; Yasuda et al., 2011, 2012). BLIMP1, however, is also a target of IRF4 (Ochiai et al., 2013; Sciammas et al., 2006) and is induced upon B cell activation and is a direct target of nuclear factor κB (NF-κB)/REL (Grumont and Gerondakis, 2000). Erk and NF-κB are both induced upon BCR and CD40 signaling in naive B cells and MBCs, and they could thus act in concert to increase IRF4 and promote PC differentiation. However, the present data and previous work from us (Szodoray et al., 2016) highlight the role of

CD45, and thus BCR signaling, in this process. Our data reveal co-expression of CD45 phosphatase activity together with BCR signaling kinases with IRF4 and BLIMP1 in MBC cultures differentiating toward ASCs, as well as the concomitant lack of induction of these transcription factors upon CD45 inhibition and silencing. However, PC differentiation is also a factor of proliferation (Tangye et al., 2003a, 2003b) and we observed a strict dependency of CD45 and Galectin-1 on Th-mediated B cell proliferation. Therefore, it is possible that Galectin-1/CD45 signaling directly promotes upregulation of IRF4 and BLIMP1; however, PC transcription factor upregulation and differentiation may be secondary to the effect observed on proliferation. These results would appear to best fit a model in which T cell help enhances CD45 phosphatase activity, BCR signaling, proliferation, and subsequent PC differentiation through induction of IRF4 and BLIMP1.

Moreover, previous studies pointed to the transmission of Th signals through the BCR (Mizuno and Rothstein, 2005; Szodoray et al., 2016), and therefore signals from T cells and the BCR may be interconnected through CD40L-mediated upregulation of CD45 phosphatase activity. In our *in vitro* studies, providing BCR cross-linking did not result in enhanced ASC differentiation; however, utilizing an inhibitor to Syk diminished ASC differentiation, demonstrating BCR signaling involvement but failing to demonstrate an advantage of acute BCR stimulation. Therefore, differentiation of PCs may be mediated by Th signal potentiation of tonic BCR signaling without requiring acute Ag stimulation of the BCR. Our data seem to fit a model of T cell-driven PC differentiation in which Th signals through CD40L-CD40 interaction upregulate Galectin-1 and CD45 activity, providing both increased acute and tonic BCR signaling capacity, leading to induction of the PC transcription factors IRF4 and BLIMP1.

Given the association between increasing T cell help and CD45 phosphatase activity in *in vitro* studies, we examined the T cell-dependent development of high-affinity PC precursors (Ise et al., 2018) and PCs in a physiological setting using a murine influenza vaccination model (Andersen et al., 2017; Grodeland et al., 2013). In agreement with our results from human cells, the highest CD45 phosphatase activity was detected in PCs. Moreover, CD45 activity within PCs correlated with Blimp1 and IRF4 expression, suggestive of CD45-mediated induction of these transcription factors. Recently, it was shown that CD40-CD40L interaction served as a dose-dependent regulator for IRF4-expressing PC precursors within the GC (Ise et al., 2018). We detected murine low- and high-affinity GC B cells based on specific Ag (HA), and IgG staining and found that such IRF4-expressing high-affinity GC PC precursors were characterized by increased CD45 phosphatase activity and therefore reinforce the link to graded T cell help and BCR affinity for antigen. These findings collectively suggest that CD45 serves as a marker of previous T cell help connecting BCR affinity with CD45 phosphatase activity and downstream PC differentiation programs.

Since neither surface expression of CD45 or CD45 isoforms could explain regulation of CD45 phosphatase activity upon stimulation with Th factors, increased availability of a CD45 ligand constitutes a feasible explanation. Our initial findings of the association between surface staining of Galectin-1 and CD45 phosphatase activity within B cells and an NA-mediated increase in both surface Galectin-1 binding and CD45 phosphatase activity suggested that Galectin-1 regulated CD45 phosphatase activity in B cells. This was

confirmed by adding recombinant human (rh)Galectin-1 protein to B cell cultures, which resulted in increased CD45 activity in Galectin-1-binding B cells. By utilizing an allosteric Galectin-1 inhibitor, OTX008, we demonstrated inhibition of Galectin-1 surface binding and T cell-mediated PC differentiation. Confocal imaging and co-immunoprecipitation experiments provided evidence for a direct association of CD45 and Galectin-1 in B cells. Lastly, ablation of *LGALS1* in Raji B cells provided definitive evidence for regulation of CD45 phosphatase activity by Galectin-1.

Galectin-1 has been suggested to regulate Ab secretion and PC differentiation in murine systems (Anginot et al., 2013; Tsai et al., 2008); however, the possibility of a connection to CD45 was not explored in these studies. It is therefore tempting to speculate that the mechanism for decreased PC differentiation in *lgals1* knockout mice is related to dysregulation of CD45 phosphatase activity. Taken together, our study connects Galectin-1 with CD45 phosphatase activity in B cells and provides a mechanism contributing to T cell-mediated PC differentiation.

We propose that T cell help imprints high CD45 phosphatase activity in B cells by enhanced surface Galectin-1 binding and that additional T cell stimulation during recall responses further increases CD45 phosphatase activity, leading to an enhanced propensity for PC differentiation capacity. Further understanding the mechanisms regulating CD45 phosphatase activity may prove important in understanding immunity to infection and development of vaccines.

STAR★METHODS

RESOURCE AVAILABILITY

Lead contact—Further information and requests for resources and reagents should be directed to and will be fulfilled by the lead contact, Peter Szodoray (peter.szodoray@medisin.uio.no).

Materials availability—Crispr/CAS9 cell lines generated in this study will be provided upon request to Peter Szodoray (peter.szodoray@medisin.uio.no).

Data and code availability—All data reported in this paper will be shared by the lead contact upon request.

This paper does not report original code.

Any additional information required to reanalyze the data reported in this paper is available from the lead contact upon request.

EXPERIMENTAL MODEL AND SUBJECT DETAILS

Human samples—Buffy coat samples were obtained from healthy adult blood donors. Bone marrow was obtained from patients undergoing routine hip replacement surgery. Ethical approval was obtained from the Regional Ethics Committee in South-Eastern

Norway (2014/840/REK and 2016/905/REK). Informed consent was obtained from all subjects prior to donation.

Mice—Six to eight weeks old female BALB/c mice (Janvier, le Genest-Saint-Isle, France) housed in a Minimal Disease Unit animal facility were used. The *in vivo* procedures were pre-approved by the Norwegian Food Safety Authority.

METHOD DETAILS

Mice, immunizations, and stimulations—DNA vaccines encoding hemagglutinin (HA) (PR8) targeted to MHCII in mice is described previously (Grodeland et al., 2013). The DNA vaccine was purified by QIAGEN EndoFree Plasmid Maxi Kit (QIAGEN) and dissolved in sterile injection fluid (0.9%NaCl). Mice were anesthetized by intraperitoneal injection of 10μl/g body weight ZRF cocktail [Zoletil Forte (250 mg/ml) (Virbac France), Rompun (20 mg/ml), (Bayer Animal Health GmbH), and Fentanyl (50 μg/ml) (Actavis, Germany)]. Mice were shaved on the lower back and received intradermal injections of 25μl with 12.5μg plasmid DNA on each flank (total DNA/mouse 25μg) followed by electroporation over the injection site (DermaVax, Cellectis, Paris, France). Four weeks after immunization, draining lymph nodes (LNs) (inguinal) and bone marrow (BM) from both tibia and femur were harvested and single cell suspensions were prepared. PR8 protein with a carboxy terminal 6x histidine tag (HA-His) was expressed and purified as described and used at 50nM concentration (Andersen et al., 2019).

Spleens were harvested from BALB/c mice and single cell suspensions were prepared by manual crushing followed by DNase and collagenase and ACK treatment to remove erythrocytes. B cells were enriched by negative selection using anti-mouse CD43 (Untouched™ B Cells) kit. Murine B cells were stimulated for 7 days with murine CD40L recombinant murine IL-4 (20 ng/ml) and IL-21 (50 ng/ml), intracellularly stained for IRF4-ALX488, Blimp1-PE and analyzed by flow cytometry.

Cell preparations—Peripheral naive and memory B cells were purified from buffy coats derived from healthy donors by utilizing the Human Memory B cell Isolation Kit (Miltenyi Biotec). For isolation of PD-L2+ MBCs, untouched switched MBCs were isolated using the Switched memory B cell Isolation Kit (Miltenyi Biotec) before PD-L2+ MBCs were further isolated using anti PD-L2 biotin and anti-Biotin Microbeads (Miltenyi Biotec). Total human B cells were isolated using CD19 Microbeads (Miltenyi Biotec). Resultant B cells were routinely checked for purity by flow cytometry staining and analysis for CD27, IgD, CD19, IgG and IgM. The isolated naive and memory B cell subsets were > 98% pure and naive B cells contained less than 0.5% $CD27^+$ B cells.

Cell culture and stimulations—Purified naive and memory B cells were cultured at 2.5×10^6 cells/ml in 200μl volume in RPMI 1640+GlutaMAX™-1 (Life Technologies) supplemented with endotoxin and mycoplasma tested 10% heat inactivated fetal bovine serum (Biochrom AG), and penicillin/streptomycin. Recombinant human IL-4 (20 ng/ml), IL-21 (50 ng/ml) (Peprotech) and soluble recombinant human CD40L (100ng/ml) (MegaCD40L, Enzo LifeSciences) were used as Th factors that were provided to purified B

cells for 48h prior to phosphoflow experiments or CD45 phosphatase activity measurements. In some experiments, hrGAL-1 (Novus Biologicals) was used at 5mg/ml. For differentiation toward ASCs, CD138-depleted naive and memory B cells were cultured (0.25×10^6 cells/well) in the presence of CD40L (50–500 ng/ml) and IL-4/IL-21 (Peprotech) for 7 days. The inhibitors PTP CD45 Inhibitor (Calbiochem), Calixarene OTX008 (Axon Medchem) or Fostamatinib (R406) (Selleckchem) were used at 1.25–5μM, 10–100μM and 5 μM during cell culture, respectively, and equal volumes of vehicle (DMSO/EtOH, EtOH, DMSO) was supplied in the other wells. In some wells BCRs were crosslinked by adding a total of 5mg/ml each of $F(ab')_2$ goat anti-human κ/λ (Southern Biotech) were supplied. Fixable Viability stain 510 (BD Biosciences) was used to exclude dead cells from analyses. Human B cells were stimulated for 2 days using The Human TLR1–9 Agonist Kit (Invivogen) according to manufacturer's recommendations. MyD88 inhibitor (Pepinh-MYD, Invivogen) was used at 5μM.

Flow cytometry—Cells were washed in FACS wash buffer (PBS/2%FBS/0.1% NaN_3) before Fc receptors were blocked using the Human FcR Blocking Reagent (Miltenyi Biotec) according to the manufacturer's description. Cells were stained with anti-human monoclonal antibodies on ice before cells were washed twice in FACS wash and once in PBS/0.1% NaN_3. In some experiments, cells were fixed using 2% paraformaldehyde/PBS (wt/vol). For detection of intracellular BLIMP1 and IRF4 expression, the BD PharMingen™ Transcription Buffer Set (BD Biosciences) was used. Flow cytometry analyses were performed using either FACS Canto II (BD Biosciences) or Attune NxT (ThermoFisher Scientific) flow cytometers and software analyses were performed using the FlowJo Cytometric software (TreeStar Inc.).

Phosphoflow analysis—Cells were equilibrated to 37°C and BCRs were crosslinked by adding a total of 10μg/ml each of $F(ab')_2$ goat anti-human κ/λ (Southern Biotech). Cells were fixed using 2% paraformaldehyde/PBS at room temperature for 10 minutes and subsequently permeabilized by adding cold 100% methanol and incubating 20 minutes at 4°C. Cells were washed twice before incubation with phospho-specific antibodies at room temperature for 1 hour. Washed cells were acquired on FACS Canto II (BD Biosciences) or Attune Nxt (Thermo Fisher Scientific) flow cytometers.

Flow cytometry-based CD45 phosphatase activity assay—A method to quantitate CD45 phosphatase activity at the single-cell level is previously described (Stanford et al., 2012). The assay takes advantage of the fluorogenic properties of phosphorylated coumaryl amino propionic acid (pCAP), an analog of phosphotyrosine, which can be incorporated into peptides (Mitra and Barrios, 2005). Once delivered into cells, pCAP peptides are dephosphorylated by protein tyrosine phosphatases, and the resulting cell fluorescence can be monitored by flow cytometry. A cell-permeable pCAP peptide specific for CD45 phosphatase activity was designed taking advantage of peptide sequences of known CD45 substrates (Stanford et al., 2012). For the cell-permeable pCAP-peptide based assay, naive and memory human B cells were isolated, cultured and stimulated as described above. Cells were harvested and washed in RPMI medium (without phenol red) supplemented with 0.5% FBS and equilibrated to 37°C before incubation with pCAP-SP1 at 2.5μM for 15 min at

37°C. Cells were washed in FACS wash supplemented with 10mM sodium orthovanadate to inhibit tyrosine phosphatase activity. Cells were then stained with surface markers on ice for 40 min and fixed in 2% paraformaldehyde (wt/vol) for 15 min at room temperature. Alternatively, CD45 activity measurement was combined with detection of intracellular markers using the BD PharMingen™ Transcription Factor Buffer Set (BD Biosciences). CD45 phosphatase activity was measured as cell fluorescence using a FACS CantoII (BD Biosciences) or Attune NxT (ThermoFisher) flow cytometers with excitation with the violet laser at 405 nm and detection with a Pacific Blue emission filter.

Quantitative real-time PCR—Total RNA was isolated from cultured purified naive and memory B cells using TRI reagent (Sigma Aldrich). Reverse transcription and quantitative PCR was performed using the Taqman®RNA-to-C_T™ 1-Step Kit (LifeTechnologies) on the StepOnePlus™ System (Life Technologies): Reverse transcription at 48°C for 15 min, then 10 min at 95°C, followed by 40 cycles at 95°C for 15 s and 1 min at 60°C in 15 μl reaction volumes with 5ng RNA as template/well. All PCR reactions were done in triplicates. Controls containing no template or no RT enzyme were included in each run. Taqman gene expression assays (ThermoFisher) were chosen that did not amplify genomic DNA. Gene expression was quantified by the comparative threshold cycle method and normalized to human *POLR2A* expression as housekeeping gene. Values are expressed as means ± SEM.

Gene silencing using siRNA—Purified total B cells (1×10^6) were resuspended in 100 μL Nucleofector®Solution at room temperature (Human B Cell Nucleofector Kit, Lonza) before 500nM siRNA directed toward CD45 or CTR siRNA (Silencer®Select Pre-designed siRNA, Ambion) were added. siRNAs were delivered by Nucleofector®Program U-015. Pre-heated culture medium were quickly added before plating in 96-well plates and stimulated with IL-21, IL-4 and CD40L as described above. Cells were harvested and stained after 7 days of stimulation.

Enzyme-linked immunosorbent assays—Human IgM and Human IgG ELISA kits (Invitrogen) were used according to the manufacturer's instructions. 50 μl naive- or memory B cell conditioned cell culture samples in RPMI were added 25 μL assay buffer and diluted in three further steps (dilution range 1:1.5–1:40.5) before applying on coated plates. Standard curves were established in duplicates ranging from 16 to 1000 ng/ml for IgM and 1.6–100 ng/ml for IgG detection. Plates were probed with HRP-conjugated secondary antibodies and signal was detected using tetramethylbenzidine substrate solution. Plates were read at read at 450 nm in a Wallac Envision 2104 Multilabel Reader (Perkin Elmer) and absorbance values were recorded using the Wallac Envision Manager 1.12 software.

For determination of murine anti-HA antibodies, blood was harvested by puncture of the saphenous vein, and sera prepared by two successive centrifugations at 17.000 × g for 5 min at room temperature. ELISA plates (Costar 3590, Corning, NY, USA) were coated with 0.5μg/ml recombinant HA [A/Puerto Rico/8/34 (H1N1)] (11684-V08H, Sino Biological, North Wales, PA, USA) overnight at 4°C. Serum antibodies were detected with alkaline phosphatase conjugated goat anti-mouse IgG (Sigma-Aldrich) at 1:5000 dilution, and developed with phosphatase substrate (Sigma-Aldrich).

Immunostaining and confocal microscopy—Following B cell isolation, cells were incubated with 10μM pCAP-SP1 peptide for 4 min at 37°C in RPMI medium (without phenol red) supplemented with 0.5% FBS. Phosphatase activity was quenched and cells fixed for 10 minutes in 10mM sodium orthovanadate/2% PFA and washed twice with PBS. Fixed cells could be adhered to Superfrost Plus microscopy slides (Thermo Fischer) via centrifugation (Shandon Cytospin 4, Thermo Scientific) at 800 rpm for 4 minutes. Prior to staining, slides dried overnight at 4°C. Permeabilization of adherent B cells was achieved by 15 minutes of incubation in a perm/wash buffer obtained from Transcription Factor Buffer Set (BD PharMingen) optimized for immunofluorescent staining. Primary antibodies were diluted in the perm/wash buffer, CD45 (1:100, BioLegend), Galectin-1 (1:25, R&D Systems), pSyk Alexa647 (1:50, Cell Signaling), and applied to B cells for 1 hour at 37°C. Cells were washed three times and incubated at room temperature in Alexa Fluor (488, 555; 1:500 in perm/wash buffer) conjugated secondary antibodies for 45 minutes. Excess secondary was washed off and labeled cells mounted with ProLong Gold Antifade (Molecular Probes). After drying, slides were sealed with nail polish and images acquired sequentially on an Olympus FV1000 confocal microscope equipped with a 60xNA1.35 UPlanSAPO oil objective. Image processing and adjustments was performed using ImageJ (National Institutes of Health) and Adobe Photoshop, with final assembly in Adobe Illustrator. Fluorescence intensities were measured with RGB profiles tool in ImageJ, values corrected for background fluorescence, normalized to the lowest value, and data was analyzed and assembled using GraphPad Prism 6.

Co-immunoprecipitation—B cells were isolated using CD19 Microbeads (Miltenyi Biotec) and cultured at 2.5×10^6 cells/ml for 48h in the presence of soluble recombinant human CD40L (100ng/ml) (MegaCD40L, Enzo LifeSciences) or PBS as control before cells were lysed using ice cold IP Lysis Buffer (Pierce) in the presence of protease inhibitors. 500 μg protein lysate was used for each IP using the Immunoprecipitation Kit Dynabeads® Protein G (Life Technologies). Briefly, 5 μg mAb (CD45, clone F10–89-4) or isotype control (mouse IgG2a, BioRad) was bound to 50 μL Dynabeads and crosslinked using BS3 reagent (ThermoFisher) according to manufacturers instructions, before cell lysate was added at 4°C for 4h. Beads were washed and bound protein was eluted and sample buffer (NuPAGE LDS sample buffer) and DTT was added. Samples were heated to 70°C for 10 min before loaded onto SDS-PAGE. Gels were transferred to polyvinylidene difluoride membrane (Bio-Rad) and blocked in 5% nonfat dry milk and 0.1% Tween. The membrane was probed with goat anti-Galectin-1 polyclonal antibody (1:2000)(R&D Systems) and anti-goat IgG HRP (1:1000)(R&D Systems) or anti-CD45 (1:1000) and anti-mouse IgG HRP (1:1000) (R&D Systems).

CRISPR-Cas9 knockdown—CRISPR-Cas9 knock-out of human and murine cell lines was performed as previously described (Tveita et al., 2016). In brief, ablation of the LGALS1 gene from the Raji cell line was achieved by electroporation of target cells with the Neon Transfection system (Thermo Fischer) using the Cas9/gRNA vector pSpCas9(BB)-2A-GFP (PX458), generously provided by Dr. Feng Zhang through the Addgene repository (Addgene #48138) utilizing the following guide RNA template sequence: hCD45: 5′-TGGCTTAAACTCTTGGCATT-3′, hLGALS_s1: 5′-CGCCGTGGGCGTTGAAGCGA-3′.

GFP-expressing cells were sorted after 24 h using FACS (BD FACSAria II cell sorter; BD Biosciences), and screened for CD45 and Galectin-1 expression by western blot analysis. CD45 phosphatase activity was measured by flow cytometry.

QUANTIFICATION AND STATISTICAL ANALYSIS

All statistical analyses were performed using Prism (GraphPad Software Inc, La Jolla, CA, USA). Where appropriate, datasets were analyzed with the D'Agostino-Pearson omnibus normality test or the Shapiro-Wilk's normality test to evaluate distribution of data. For normally distributed data, the comparison of variables was performed using one-way ANOVA or repeated-measures (RM) one-way ANOVA for unpaired or paired data, respectively, followed by Tukey's, Sidak's or Dunnett's multiple comparison tests. For not normally distributed data, the comparison of variables was performed using Kruskal-Wallis test or Friedman test for unpaired and paired data, respectively, followed by Dunn's multiple comparison test. For the comparison of two variables, the paired Student's t test was used for normally distributed data and the Wilcoxon matched-pairs signed rank test was used for not normally distributed datasets. $p < 0.05$ was considered statistically significant. Data are represented as means ± SEM.* $p < 0.05$, ** $p < 0.01$, *** $p < 0.001$, **** $p < 0.0001$.

Supplementary Material

Refer to Web version on PubMed Central for supplementary material.

ACKNOWLEDGMENTS

This work was supported by the Stiftelsen Kristian Gerhard Jebsen (grant no. SKGJ-MED-019), the Research Council of Norway through its Centers of Excellence funding scheme (project no. 179573/V40), the Norwegian Cancer Society, the South-Eastern Norway Regional Health Authority (grant nos. 2011018 and 2021066), the University of Oslo, the Oslo University Hospital-Rikshospitalet, UNIFOR funds by the University of Oslo, and Odd Fellow Norway (to P.S. and B.N.), as well as by National Institutes of Health grant AI070544 (to N.B.) and American Diabetes Association Pathway Initiator Award 1–15-INI-13 (to S.M.S.). The authors would like to thank the Blood Bank and the Confocal Microscopy and Flow Cytometry Core Facilities at the Oslo University Hospital and Dr. Liv T.N. Osnes for expert help with immunophenotyping.

REFERENCES

Aiba Y, Kometani K, Hamadate M, Moriyama S, Sakaue-Sawano A, Tomura M, Luche H, Fehling HJ, Casellas R, Kanagawa O., et al. (2010). Preferential localization of IgG memory B cells adjacent to contracted germinal centers. Proc. Natl. Acad. Sci. USA 107, 12192–12197. [PubMed: 20547847]

Alhabbab R, Blair P, Smyth LA, Ratnasothy K, Peng Q, Moreau A, Lechler R, Elgueta R, and Lombardi G. (2018). Galectin-1 is required for the regulatory function of B cells. Sci. Rep8, 2725. [PubMed: 29426942]

Allen CD, Okada T, Tang HL, and Cyster JG (2007). Imaging of germinal center selection events during affinity maturation. Science 315, 528–531. [PubMed: 17185562]

Amano M, Galvan M, He J, and Baum LG (2003). The ST6Gal I sialyltransferase selectively modifies *N*-glycans on CD45 to negatively regulate galectin-1-induced CD45 clustering, phosphatase modulation, and T cell death. J. Biol. Chem 278, 7469–7475. [PubMed: 12499376]

Andersen TK, Zhou F, Cox R, Bogen B, and Grødeland G. (2017). A DNA vaccine that targets hemagglutinin to antigen-presenting cells protects mice against H7 influenza. J. Virol91, e01340–17. [PubMed: 28931687]

Andersen TK, Huszthy PC, Gopalakrishnan RP, Jacobsen JT, Fauskanger M, Tveita AA, Grødeland G, and Bogen B. (2019). Enhanced germinal center reaction by targeting vaccine antigen to major histocompatibility complex class II molecules. NPJ Vaccines4, 9. [PubMed: 30775000]

Anginot A, Espeli M, Chasson L, Mancini SJ, and Schiff C. (2013). Galectin 1 modulates plasma cell homeostasis and regulates the humoral immune response. J. Immunol190, 5526–5533. [PubMed: 23616571]

Arpin C, Banchereau J, and Liu YJ (1997). Memory B cells are biased towards terminal differentiation: A strategy that may prevent repertoire freezing. J. Exp. Med 186, 931–940. [PubMed: 9294147]

Astorgues-Xerri L, Riveiro ME, Tijeras-Raballand A, Serova M, Rabinovich GA, Bieche I, Vidaud M, de Gramont A, Martinet M, Cvitkovic E., et al. (2014). OTX008, a selective small-molecule inhibitor of galectin-1, downregulates cancer cell proliferation, invasion and tumour angiogenesis. Eur. J. Cancer 50, 2463–2477. [PubMed: 25042151]

Benson MJ, Elgueta R, Schpero W, Molloy M, Zhang W, Usherwood E, and Noelle RJ (2009). Distinction of the memory B cell response to cognate antigen versus bystander inflammatory signals. J. Exp. Med 206, 2013–2025. [PubMed: 19703988]

Berkowska MA, Driessen GJ, Bikos V, Grosserichter-Wagener C, Stamatopoulos K, Cerutti A, He B, Biermann K, Lange JF, van der Burg M., et al. (2011). Human memory B cells originate from three distinct germinal center-dependent and -independent maturation pathways. Blood 118, 2150–2158. [PubMed: 21690558]

Bonzi J, Bornet O, Betzi S, Kasper BT, Mahal LK, Mancini SJ, Schiff C, Sebban-Kreuzer C, Guerlesquin F, and Elantak L. (2015). Pre-B cell receptor binding to galectin-1 modifies galectin-1/carbohydrate affinity to modulate specific galectin-1/glycan lattice interactions. Nat. Commun6, 6194. [PubMed: 25708191]

Cao A, Alluqmani N, Buhari FHM, Wasim L, Smith LK, Quaile AT, Shannon M, Hakim Z, Furmli H, Owen DM, et al. (2018). Galectin-9 binds IgM-BCR to regulate B cell signaling. Nat. Commun 9, 3288. [PubMed: 30120235]

Croci DO, Morande PE, Dergan-Dylon S, Borge M, Toscano MA, Stupirski JC, Bezares RF, Avalos JS, Narbaitz M, Gamberale R., et al. (2013). Nurse-like cells control the activity of chronic lymphocytic leukemia B cells via galectin-1. Leukemia 27, 1413–1416. [PubMed: 23257714]

Cyster JG, Healy JI, Kishihara K, Mak TW, Thomas ML, and Good-now CC (1996). Regulation of B-lymphocyte negative and positive selection by tyrosine phosphatase CD45. Nature 381, 325–328. [PubMed: 8692271]

Davey AM, and Pierce SK (2012). Intrinsic differences in the initiation of B cell receptor signaling favor responses of human IgG^+ memory B cells over IgM^+ naive B cells. J. Immunol 188, 3332–3341. [PubMed: 22379037]

Dings RP, Miller MC, Nesmelova I, Astorgues-Xerri L, Kumar N, Serova M, Chen X, Raymond E, Hoye TR, and Mayo KH (2012). Antitumor agent calixarene 0118 targets human galectin-1 as an allosteric inhibitor of carbohydrate binding. J. Med. Chem 55, 5121–5129. [PubMed: 22575017]

Dogan I, Bertocci B, Vilmont V, Delbos F, Megret J, Storck S, Reynaud CA, and Weill JC (2009). Multiple layers of B cell memory with different effector functions. Nat. Immunol 10, 1292–1299. [PubMed: 19855380]

Earl LA, Bi S, and Baum LG (2010). *N*- and *O*-glycans modulate galectin-1 binding, CD45 signaling, and T cell death. J. Biol. Chem 285, 2232–2244. [PubMed: 19920154]

Elantak L, Espeli M, Boned A, Bornet O, Bonzi J, Gauthier L, Feracci M, Roche P, Guerlesquin F, and Schiff C. (2012). Structural basis for galectin-1-dependent pre-B cell receptor (pre-BCR) activation. J. Biol. Chem287, 44703–44713. [PubMed: 23124203]

Espeli M, Mancini SJ, Breton C, Poirier F, and Schiff C. (2009). Impaired B-cell development at the pre-BII-cell stage in galectin-1-deficient mice due to inefficient pre-BII/stromal cell interactions. Blood113, 5878–5886. [PubMed: 19329777]

Fouillit M, Joubert-Caron R, Poirier F, Bourin P, Monostori E, Levi-Strauss M, Raphael M, Bladier D, and Caron M. (2000). Regulation of CD45-induced signaling by galectin-1 in Burkitt lymphoma B cells. Glycobiology10, 413–419. [PubMed: 10764829]

Giovannone N, Liang J, Antonopoulos A, Geddes Sweeney J, King SL, Pochebit SM, Bhattacharyya N, Lee GS, Dell A, Widlund HR, et al. (2018). Galectin-9 suppresses B cell receptor signaling and is regulated by Ibranching of N-glycans. Nat. Commun 9, 3287. [PubMed: 30120234]

Gitlin AD, von Boehmer L, Gazumyan A, Shulman Z, Oliveira TY, and Nussenzweig MC (2016). Independent roles of switching and hypermutation in the development and persistence of B lymphocyte memory. Immunity 44, 769–781. [PubMed: 26944202]

Grodeland G, Mjaaland S, Roux KH, Fredriksen AB, and Bogen B. (2013). DNA vaccine that targets hemagglutinin to MHC class II molecules rapidly induces antibody-mediated protection against influenza. J. Immunol191, 3221–3231. [PubMed: 23956431]

Grumont RJ, and Gerondakis S. (2000). Rel induces interferon regulatory factor 4 (IRF-4) expression in lymphocytes: Modulation of interferon-regulated gene expression by rel/nuclear factor kappaB. J. Exp. Med191, 1281–1292. [PubMed: 10770796]

Halliley JL, Tipton CM, Liesveld J, Rosenberg AF, Darce J, Gregoretti IV, Popova L, Kaminiski D, Fucile CF, Albizua I., et al. (2015). Long-lived plasma cells are contained within the $CD19^{-}CD38^{hi}CD138^{+}$ subset in human bone marrow. Immunity 43, 132–145. [PubMed: 26187412]

Hebeis BJ, Klenovsek K, Rohwer P, Ritter U, Schneider A, Mach M, and Winkler TH (2004). Activation of virus-specific memory B cells in the absence of T cell help. J. Exp. Med 199, 593–602. [PubMed: 14769849]

Hermiston ML, Xu Z, and Weiss A. (2003). CD45: A critical regulator of signaling thresholds in immune cells. Annu. Rev. Immunol21, 107–137. [PubMed: 12414720]

Hermiston ML, Tan AL, Gupta VA, Majeti R, and Weiss A. (2005). The juxtamembrane wedge negatively regulates CD45 function in B cells. Immunity23, 635–647. [PubMed: 16356861]

Hughes RC (1999). Secretion of the galectin family of mammalian carbohydrate-binding proteins. Biochim. Biophys. Acta 1473, 172–185. [PubMed: 10580137]

Huntington ND, Xu Y, Puthalakath H, Light A, Willis SN, Strasser A, and Tarlinton DM (2006). CD45 links the B cell receptor with cell survival and is required for the persistence of germinal centers. Nat. Immunol 7, 190–198. [PubMed: 16378097]

Inagaki Y, Hayakawa F, Hirano D, Kojima Y, Morishita T, Yasuda T, Naoe T, and Kiyoi H. (2016). PAX5 tyrosine phosphorylation by SYK co-operatively functions with its serine phosphorylation to cancel the PAX5-dependent repression of BLIMP1: A mechanism for antigen-triggered plasma cell differentiation. Biochem. Biophys. Res. Commun475, 176–181. [PubMed: 27181361]

Ise W, Fujii K, Shiroguchi K, Ito A, Kometani K, Takeda K, Kawakami E, Yamashita K, Suzuki K, Okada T, and Kurosaki T. (2018). T follicular helper cell-germinal center B cell interaction strength regulates entry into plasma cell or recycling germinal center cell fate. Immunity48, 702–715.e4. [PubMed: 29669250]

Khalil AM, Cambier JC, and Shlomchik MJ (2012). B cell receptor signal transduction in the GC is short-circuited by high phosphatase activity. Science 336, 1178–1181. [PubMed: 22555432]

Klein U, Casola S, Cattoretti G, Shen Q, Lia M, Mo T, Ludwig T, Rajewsky K, and Dalla-Favera R. (2006). Transcription factor IRF4 controls plasma cell differentiation and class-switch recombination. Nat. Immunol7, 773–782. [PubMed: 16767092]

Koethe S, Zander L, Köster S, Annan A, Ebenfelt A, Spencer J, and Bemark M. (2011). Pivotal advance: CD45RB glycosylation is specifically regulated during human peripheral B cell differentiation. J. Leukoc. Biol90, 5–19. [PubMed: 21278234]

Kometani K, Nakagawa R, Shinnakasu R, Kaji T, Rybouchkin A, Moriyama S, Furukawa K, Koseki H, Takemori T, and Kurosaki T. (2013). Repression of the transcription factor Bach2 contributes to predisposition of IgG1 memory B cells toward plasma cell differentiation. Immunity39, 136–147. [PubMed: 23850379]

Kräutler NJ, Suan D, Butt D, Bourne K, Hermes JR, Chan TD, Sundling C, Kaplan W, Schofield P, Jackson J., et al. (2017). Differentiation of germinal center B cells into plasma cells is initiated by high-affinity antigen and completed by Tfh cells. J. Exp. Med 214, 1259–1267. [PubMed: 28363897]

Kurosaki T, Kometani K, and Ise W. (2015). Memory B cells. Nat. Rev. Immunol15, 149–159. [PubMed: 25677494]

Li X, Gadzinsky A, Gong L, Tong H, Calderon V, Li Y, Kitamura D, Klein U, Langdon WY, Hou F., et al. (2018). Cbl ubiquitin ligases control B cell exit from the germinal-center reaction. Immunity 48, 530–541.e6. [PubMed: 29562201]

Lutz J, Dittmann K, Bösl MR, Winkler TH, Wienands J, and Engels N. (2015). Reactivation of IgG-switched memory B cells by BCR-intrinsic signal amplification promotes IgG antibody production. Nat. Commun6, 8575. [PubMed: 26815242]

McHeyzer-Williams M, Okitsu S, Wang N, and McHeyzer-Williams L. (2011). Molecular programming of B cell memory. Nat. Rev. Immunol12, 24–34. [PubMed: 22158414]

Mei HE, Wirries I, Frölich D, Brisslert M, Giesecke C, Grün JR, Alexander T, Schmidt S, Luda K, Kühl AA, et al. (2015). A unique population of IgG-expressing plasma cells lacking CD19 is enriched in human bone marrow. Blood 125, 1739–1748. [PubMed: 25573986]

Mesin L, Ersching J, and Victora GD (2016). Germinal center B cell dynamics. Immunity 45, 471–482. [PubMed: 27653600]

Mitra S, and Barrios AM (2005). Highly sensitive peptide-based probes for protein tyrosine phosphatase activity utilizing a fluorogenic mimic of phosphotyrosine. Bioorg. Med. Chem. Lett 15, 5142–5145. [PubMed: 16203147]

Mizuno T, and Rothstein TL (2005). B cell receptor (BCR) cross-talk: CD40 engagement enhances BCR-induced ERK activation. J. Immunol 174, 3369–3376. [PubMed: 15749869]

Moran I, Nguyen A, Khoo WH, Butt D, Bourne K, Young C, Hermes JR, Biro M, Gracie G, Ma CS, et al. (2018). Memory B cells are reactivated in subcapsular proliferative foci of lymph nodes. Nat. Commun 9, 3372. [PubMed: 30135429]

Nguyen JT, Evans DP, Galvan M, Pace KE, Leitenberg D, Bui TN, and Baum LG (2001). CD45 modulates galectin-1-induced T cell death: Regulation by expression of core 2 *O*-glycans. J. Immunol 167, 5697–5707. [PubMed: 11698442]

Nutt SL, Hodgkin PD, Tarlinton DM, and Corcoran LM (2015). The generation of antibody-secreting plasma cells. Nat. Rev. Immunol 15, 160–171. [PubMed: 25698678]

Ochiai K, Maienschein-Cline M, Simonetti G, Chen J, Rosenthal R, Brink R, Chong AS, Klein U, Dinner AR, Singh H, and Sciammas R. (2013). Transcriptional regulation of germinal center B and plasma cell fates by dynamical control of IRF4. Immunity38, 918–929. [PubMed: 23684984]

Pape KA, Taylor JJ, Maul RW, Gearhart PJ, and Jenkins MK (2011). Different B cell populations mediate early and late memory during an endogenous immune response. Science 331, 1203–1207. [PubMed: 21310965]

Paus D, Phan TG, Chan TD, Gardam S, Basten A, and Brink R. (2006). Antigen recognition strength regulates the choice between extrafollicular plasma cell and germinal center B cell differentiation. J. Exp. Med203, 1081–1091. [PubMed: 16606676]

Paz H, Joo EJ, Chou CH, Fei F, Mayo KH, Abdel-Azim H, Ghazarian H, Groffen J, and Heisterkamp N. (2018). Treatment of B-cell precursor acute lymphoblastic leukemia with the Galectin-1 inhibitor PTX008. J. Exp. Clin. Cancer Res37, 67. [PubMed: 29580262]

Phan TG, Paus D, Chan TD, Turner ML, Nutt SL, Basten A, and Brink R. (2006). High affinity germinal center B cells are actively selected into the plasma cell compartment. J. Exp. Med203, 2419–2424. [PubMed: 17030950]

Popa SJ, Stewart SE, and Moreau K. (2018). Unconventional secretion of annexins and galectins. Semin. Cell Dev. Biol83, 42–50. [PubMed: 29501720]

Rajewsky K. (1996). Clonal selection and learning in the antibody system. Nature381, 751–758. [PubMed: 8657279]

Sciammas R, Shaffer AL, Schatz JH, Zhao H, Staudt LM, and Singh H. (2006). Graded expression of interferon regulatory factor-4 coordinates isotype switching with plasma cell differentiation. Immunity25, 225–236. [PubMed: 16919487]

Sciammas R, Li Y, Warmflash A, Song Y, Dinner AR, and Singh H. (2011). An incoherent regulatory network architecture that orchestrates B cell diversification in response to antigen signaling. Mol. Syst. Biol7, 495. [PubMed: 21613984]

Stanford SM, Panchal RG, Walker LM, Wu DJ, Falk MD, Mitra S, Damle SS, Ruble D, Kaltcheva T, Zhang S., et al. (2012). High-throughput screen using a single-cell tyrosine phosphatase assay

reveals biologically active inhibitors of tyrosine phosphatase CD45. Proc. Natl. Acad. Sci. USA 109, 13972–13977. [PubMed: 22891353]

Sundblad V, Morosi LG, Geffner JR, and Rabinovich GA (2017). Galectin-1: A jack-of-all-trades in the resolution of acute and chronic inflammation. J. Immunol 199, 3721–3730. [PubMed: 29158348]

Szodoray P, Stanford SM, Molberg Ø, Munthe LA, Bottini N, and Nakken B. (2016). T-helper signals restore B-cell receptor signaling in autoreactive anergic B cells by upregulating CD45 phosphatase activity. J. Allergy Clin. Immunol138, 839–851.e8. [PubMed: 27056269]

Tangye SG, and Tarlinton DM (2009). Memory B cells: Effectors of long-lived immune responses. Eur. J. Immunol 39, 2065–2075. [PubMed: 19637202]

Tangye SG, Ferguson A, Avery DT, Ma CS, and Hodgkin PD (2002). Isotype switching by human B cells is division-associated and regulated by cytokines. J. Immunol 169, 4298–4306. [PubMed: 12370361]

Tangye SG, Avery DT, Deenick EK, and Hodgkin PD (2003a). Intrinsic differences in the proliferation of naive and memory human B cells as a mechanism for enhanced secondary immune responses. J. Immunol 170, 686–694. [PubMed: 12517929]

Tangye SG, Avery DT, and Hodgkin PD (2003b). A division-linked mechanism for the rapid generation of Ig-secreting cells from human memory B cells. J. Immunol 170, 261–269. [PubMed: 12496408]

Tsai CM, Chiu YK, Hsu TL, Lin IY, Hsieh SL, and Lin KI (2008). Galectin-1 promotes immunoglobulin production during plasma cell differentiation. J. Immunol 181, 4570–4579. [PubMed: 18802059]

Tveita A, Fauskanger M, Bogen B, and Haabeth OA (2016). Tumor-specific $CD4^+$ T cells eradicate myeloma cells genetically deficient in MHC class II display. Oncotarget 7, 67175–67182. [PubMed: 27626487]

Victora GD, and Nussenzweig MC (2012). Germinal centers. Annu. Rev. Immunol 30, 429–457. [PubMed: 22224772]

Victora GD, Schwickert TA, Fooksman DR, Kamphorst AO, Meyer-Hermann M, Dustin ML, and Nussenzweig MC (2010). Germinal center dynamics revealed by multiphoton microscopy with a photoactivatable fluorescent reporter. Cell 143, 592–605. [PubMed: 21074050]

Yasuda T, Kometani K, Takahashi N, Imai Y, Aiba Y, and Kurosaki T. (2011). ERKs induce expression of the transcriptional repressor Blimp-1 and subsequent plasma cell differentiation. Sci. Signal4, ra25. [PubMed: 21505187]

Yasuda T, Hayakawa F, Kurahashi S, Sugimoto K, Minami Y, Tomita A, and Naoe T. (2012). B cell receptor-ERK1/2 signal cancels PAX5-dependent repression of BLIMP1 through PAX5 phosphorylation: A mechanism of antigen-triggering plasma cell differentiation. J. Immunol188, 6127–6134. [PubMed: 22593617]

Zikherman J, Doan K, Parameswaran R, Raschke W, and Weiss A. (2012). Quantitative differences in CD45 expression unmask functions for CD45 in B-cell development, tolerance, and survival. Proc. Natl. Acad. Sci. USA109, E3–E12. [PubMed: 22135465]

Zuccarino-Catania GV, Sadanand S, Weisel FJ, Tomayko MM, Meng H, Kleinstein SH, Good-Jacobson KL, and Shlomchik MJ (2014). CD80 and PD-L2 define functionally distinct memory B cell subsets that are independent of antibody isotype. Nat. Immunol 15, 631–637. [PubMed: 24880458]

Highlights

- Memory B cells (MBCs) have high CD45 phosphatase activity
- CD45 phosphatase activity defines high-affinity plasma cell precursors
- Effective ASC differentiation of MBCs depends on high CD45 phosphatase activity
- CD40L upregulates CD45 phosphatase activity through surface binding of Galectin-1

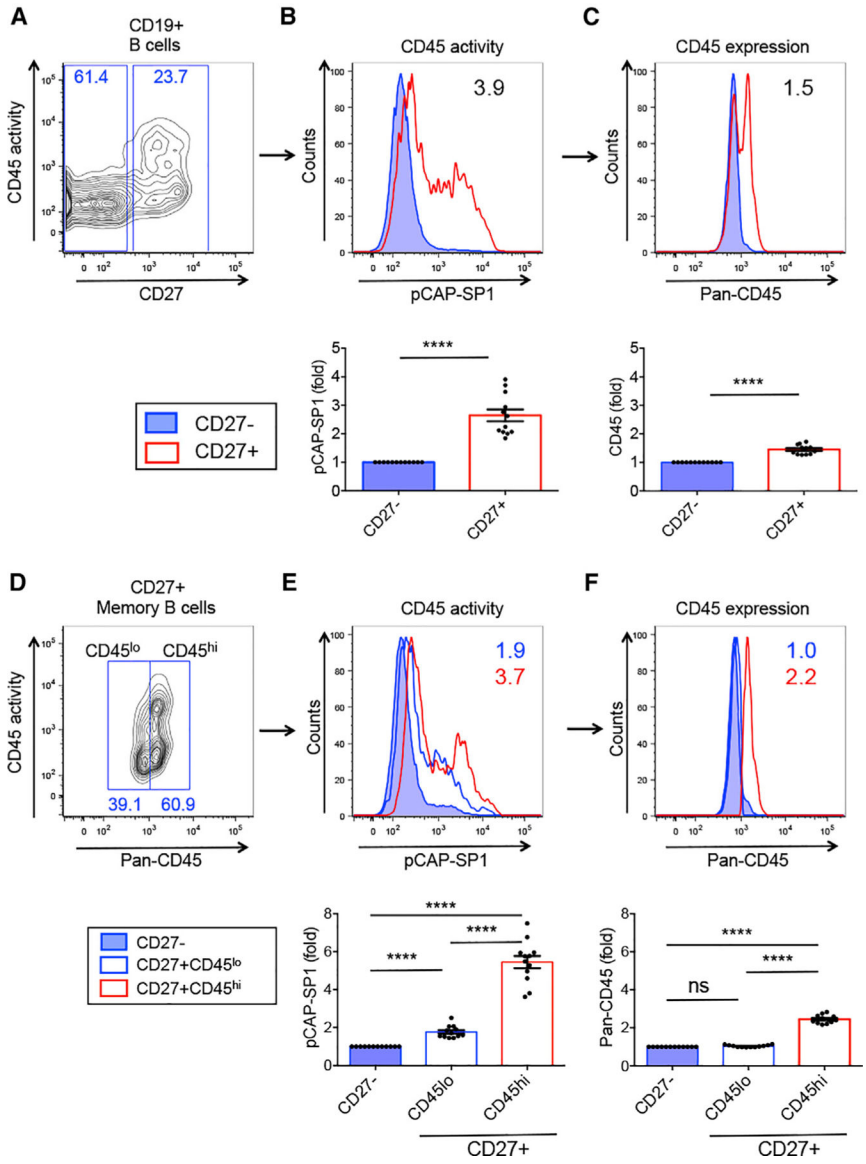

Figure 1. CD45 phosphatase activity is increased in human memory B cells

(A) Flow cytometry dot plot showing CD45 phosphatase activity versus CD27 expression on gated $CD19^+$ human peripheral B cells.

(B and C) CD45 phosphatase activity (B) and CD45 surface expression (C) of $CD27^-$ (blue) and $CD27^+$ B cells (red). Numbers in histograms represent CD45 activity (pCAP-SP1) (B) or CD45 surface expression (C) as the mean fluorescence intensity (MFI) ratio of $CD27^+$/$CD27^-$ B cells. Bottom graphs: pCAP-SP1 or CD45 surface expression (MFI) in $CD27^+$ relative to $CD27^-$ B cells.

(D) CD45 expression versus CD45 phosphatase activity in gated $CD27^+$ MBCs; $CD45^{hi}$ and $CD45^{lo}$ expression gates are shown.

(E) CD45 phosphatase activity and (F) CD45 expression in $CD27^+$ MBCs expressing low (blue open histogram) or high (red open histogram) levels of surface CD45 compared to

CD27⁻ B cells (filled blue histogram). Graphs show pCAP-SP1 or CD45 MFI relative to CD27⁻ B cells. n = 12.

Related to Figure S1. ****$p < 0.0001$.

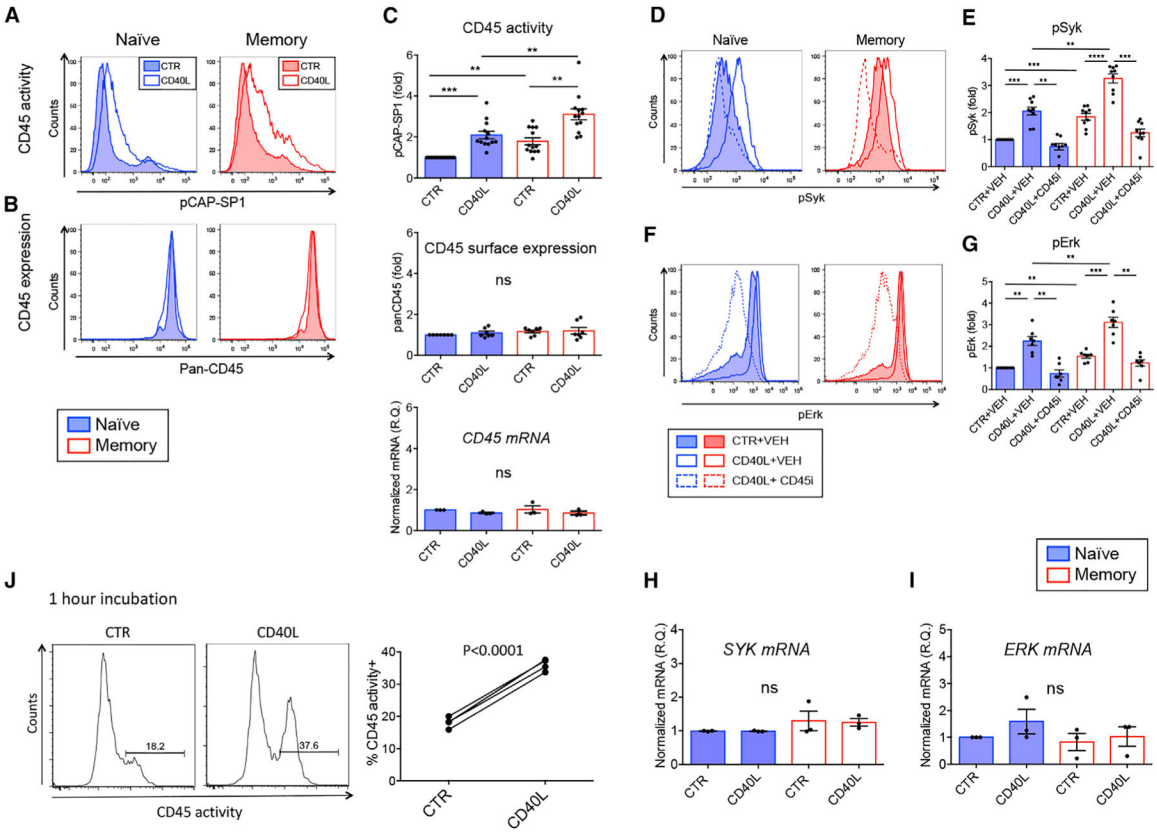

Figure 2. CD45 phosphatase activity is upregulated upon CD40L stimulation and leads to more potent BCR signaling in MBCs

(A and B) CD45 phosphatase activity (A) and CD45 surface expression (B) in naive B cells (left panels) and MBCs (right panels), control (CTR) treated (filled histogram) or CD40L (open histograms).

(C) CD45 phosphatase activity (upper panel, n = 13), panCD45 surface expression (middle panel, n= 7), and CD45 mRNA levels (lower panel, n = 3) of naive B cells (blue) and MBCs (red), CTR or CD40L treated. Graphs show pCAP-SP1 (upper panel) or CD45 (middle panel) MFI values relative to naive B cells. Lower graph: Quantitative real-time PCR of *CD45* mRNA normalized to *POLR2A* expressed as RQ (relative quantity).

(D and F) Activated BCR signaling kinases pSyk (D) and pErk (F) upon BCR cross-linking in naive B cells (left panel) or MBC (right panel) in CTR+vehicle (VEH) (filled histograms), CD40L+VEH (open histograms), or CD40L+CD45 inhibitor (open dotted histograms).

(E and G) Graphs show pSyk (n= 9) (E) and pErk (n = 7) (G) MFI values relative to CTR naive B cells.

(H and I) Real-time quantitative PCR analysis of *SYK* (H) and *ERK* (I) mRNA relative to *POLR2A* expressed as RQ (n = 3).

(J) Purified human B cells were stimulated for 1 h at 37°C before CD45 activity was measured. Graph depicts % CD45 activity^{+} B cells in CTR or CD40L-stimulated B cells (n= 4).

Related to Figure S1. **p < 0.01, ***p < 0.001, ****p < 0.0001.

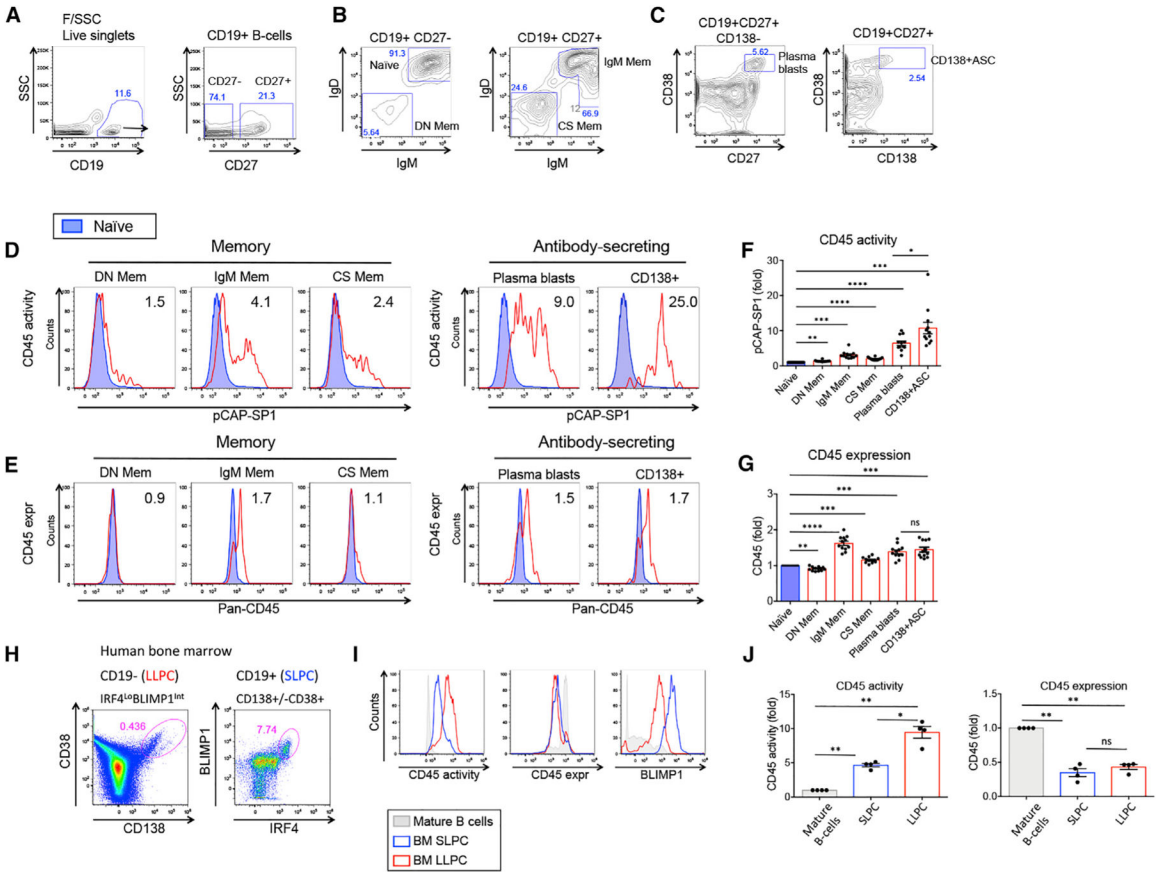

Figure 3. CD45 phosphatase activity is increased in human MBC and antibody-secreting cell subsets

(A–C) Flow cytometry dot plots showing gating of peripheral blood B cell subsets.

(D and E) CD45 phosphatase activity (D) and panCD45 surface expression (E) in human MBC and ASC subpopulations (red) compared to naive B cells (blue). Numbers in the histograms represent MFI ratio relative to naive B cells.

(F and G) Graphs show pCAP-SP1 (F) and panCD45 surface expression (G) MFI values relative to naive B cells (n= 12).

(H) Human BM $CD19^{-}CD38^{hi}CD138^{+}$ (left panel) and $CD19^{+}CD138^{+/-}CD38^{+}$ (right panel) previously shown to contain LLPCs and SLPCs, respectively.

(I) CD45 phosphatase activity (left panel), CD45 surface expression (middle panel), and BLIMP1 expression (right panel) in LLPCs (red) and SLPCs (blue) relative to mature BM B cells ($CD19^{+}SSC^{lo}CD45^{hi}$) obtained from the same donor (gray).

(J) Graphs show fold change in MFI of CD45 phosphatase activity (left panel) and CD45 surface expression (right panel) from human BM PCs relative to mature BM B cells from the same healthy donor (n = 4).

Related to Figure S2. *p < 0.05, **p < 0.01, ***p < 0.001, ****p < 0.0001.

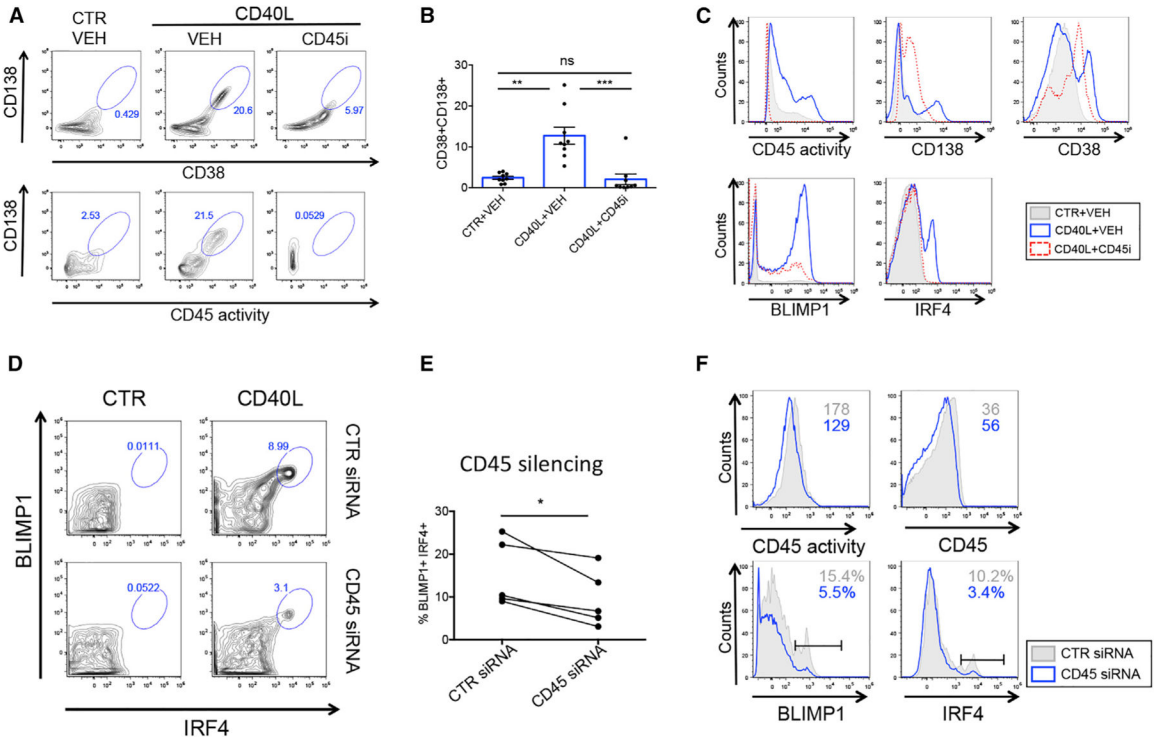

Figure 4. Differentiation of antibody-secreting cells by Th signals is CD45-dependent

(A) Flow cytometry plots show gated $CD38^{hi}CD138^{hi}$ ASCs (upper panel) and CD45 activity versus CD138 expression (lower panel) in the presence of Th signals and CD45 inhibitor as indicated.

(B) Graph shows % $CD38^{hi}CD138^{hi}$ ASC B cells (n= 8).

(C) Histograms show the CD45-dependent regulation of ASC-associated markers and transcription factors. CTR+VEH (gray), CD40L+VEH (blue), CD40L+CD45 inhibitor (red).

(D) Human peripheral B cells differentiated toward ASCs in the presence of CTR siRNA (upper panels) or CD45 siRNA (lower panels).

(E) Graph shows % $IRF4^{+}BLIMP1^{+}$ ASCs upon delivery of CTR or CD45 siRNA (n = 5).

(F) Flow cytometry histograms show expression of CD45 activity (upper left panel), CD45 surface expression (upper right panel), BLIMP1 (lower left panel), and IRF4 (lower right panel) in purified B cells differentiated toward ASCs in the presence of CTR siRNA (gray) or CD45 siRNA (blue).

Related to Figure S3. *p < 0.05, **p < 0.01, ***p < 0.001.

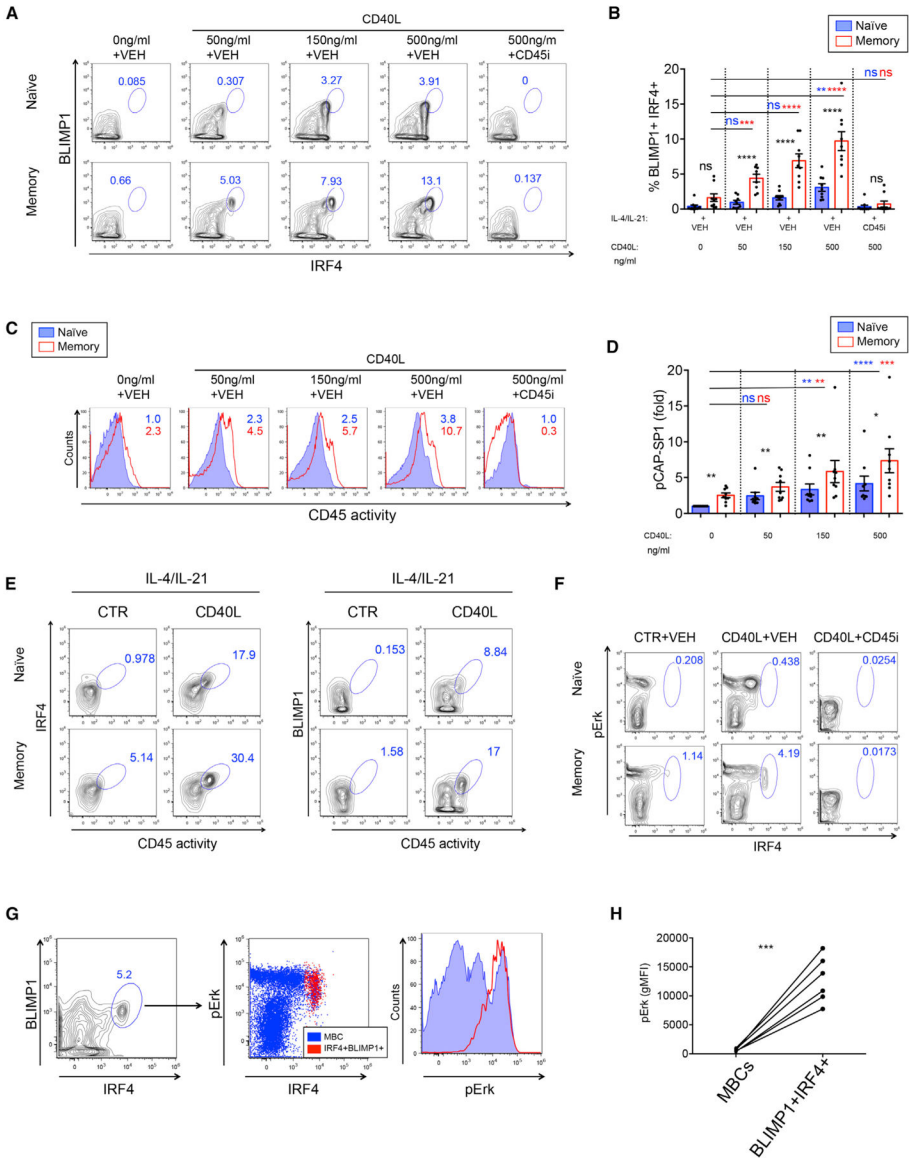

Figure 5. Increasing T cell help leads to an incremental increase in CD45 phosphatase activity and efficient MBC differentiation into ASCs

(A) Flow cytometry plots show IRF4 and BLIMP1 expression on gated live cells with increasing levels of CD40L. CD45 inhibitor was used at 1.25 μM.

(B) Graph shows % IRF4^{+}BLIMP1^{+} B cells in naive (blue) and memory (red) B cell cultures. Black asterisks represent significant differences between naive B cells and MBCs. Blue and red asterisks represent significant differences in naive B cells or MBCs stimulated with increasing concentrations of CD40L, respectively (n=9).

(C) CD45 phosphatase activity in naive B cells (blue) and MBCs (red) upon incremental concentrations of CD40L.

(D) Graph shows fold increase in MFI of CD45 phosphatase activity relative to naive unstimulated B cells (n = 9).

(E) Flow cytometry plots show co-expression of CD45 phosphatase activity and expression of PC transcription factors IRF4 and BLIMP1 in naive B cells and MBCs upon provision of Th signals or CTR-treated B cells.
(F) Flow cytometry plot showing co-expression of pErk and IRF4 in MBCs differentiated toward ASCs.
(G) Dot plot shows $IRF4^+BLIMP1^+$ ASCs (left panel) backgating to $IRF4^+pErk^+$ cells (red) compared to overall MBCs (blue) (middle panel). Right panel: Histogram shows expression of pErk in $IRF4^+BLIMP1^+$ ASCs (red) compared to total MBCs (blue).
(H) Graph shows pErk MFI values in MBCs and $IRF4^+BLIMP1^+$ ASCs (n = 6).
Related to Figures S3–S5. *p < 0.05, **p < 0.01, ***p < 0.001, ****p < 0.0001.

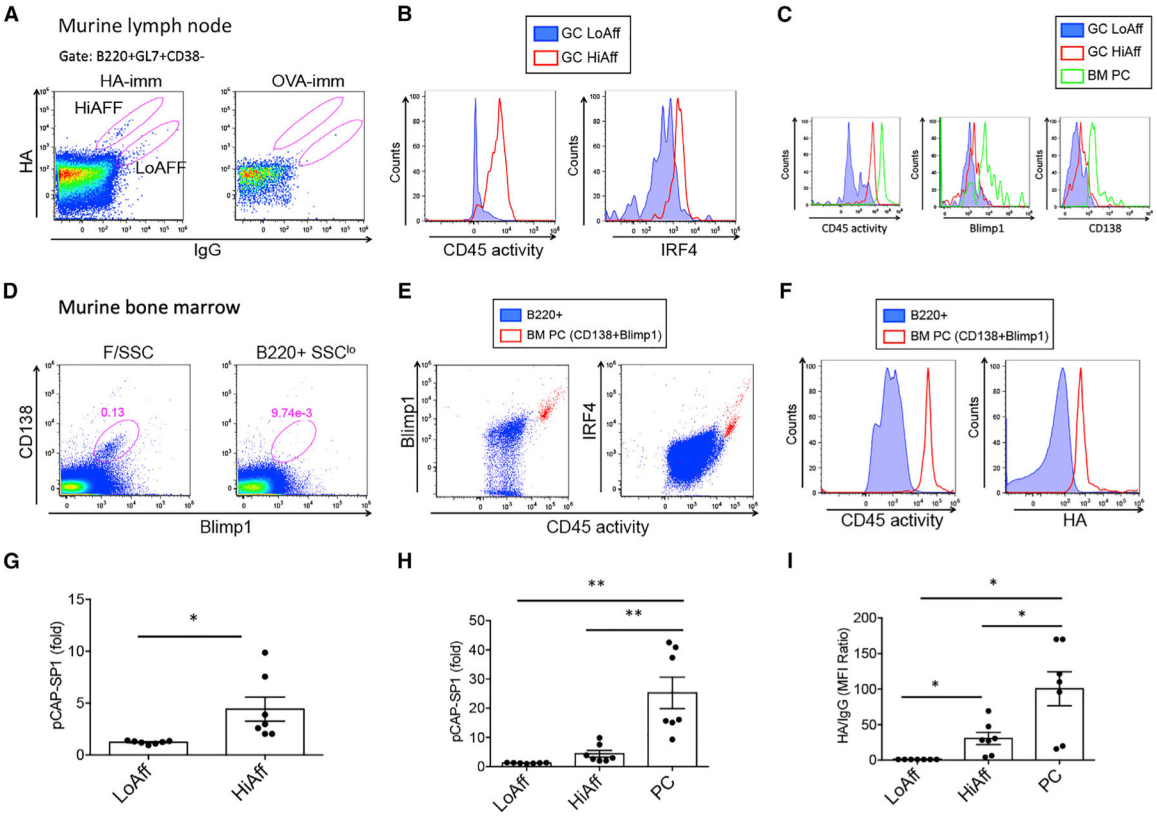

Figure 6. CD45 phosphatase activity defines high-affinity germinal center (GC) PC precursors in a T cell-dependent vaccination system

(A) Representative dot plots showing LN GC B cells ($B220^{+}GL7^{+}CD38^{-}$) and high- and low-affinity HA-reactive cells; HA binding versus IgG expression is shown.

(B) Histograms show CD45 activity (left) and IRF4 expression (right) in GC low- (blue-filled histograms) and high-affinity (red) B cells.

(C) BM PCs gated as $Blimp1^{+}CD138^{+}$ cells (green) overlayed on histograms of low- (blue) and high-affinity (red) GC B cells showing CD45 activity (left) and Blimp1 (middle) and CD138 (right) expression levels.

(D) Dot plots show BM PC gate from forward and side scatter (F/SSC)-gated cells (left) and from $B220^{+}SSC^{lo}$-gated cells (right).

(E) PCs were backgated on dot plots depicting CD45 activity and Blimp1 (left) and CD45 activity and IRF4 (right); PCs are depicted as red dots, BM $B220^{+}$ B cells are represented in blue.

(F) PCs (red) and $B220^{+}$ B cells (blue) were analyzed for CD45 activity (left) and HA binding (right).

(G and H) Graphs show MFI of CD45 activity of low-affinity (LoAff) and high-affinity (HiAff) GC B cells and BM PCs relative to $B220^{+}$ B cells within the same sample (LN or BM).

(I) Graph shows MFI ratio of HA normalized to IgG. Data are representative of two experiments including seven immunized mice in addition to immunization and staining controls.

Related to Figure S6. *$p < 0.05$, **$p < 0.01$.

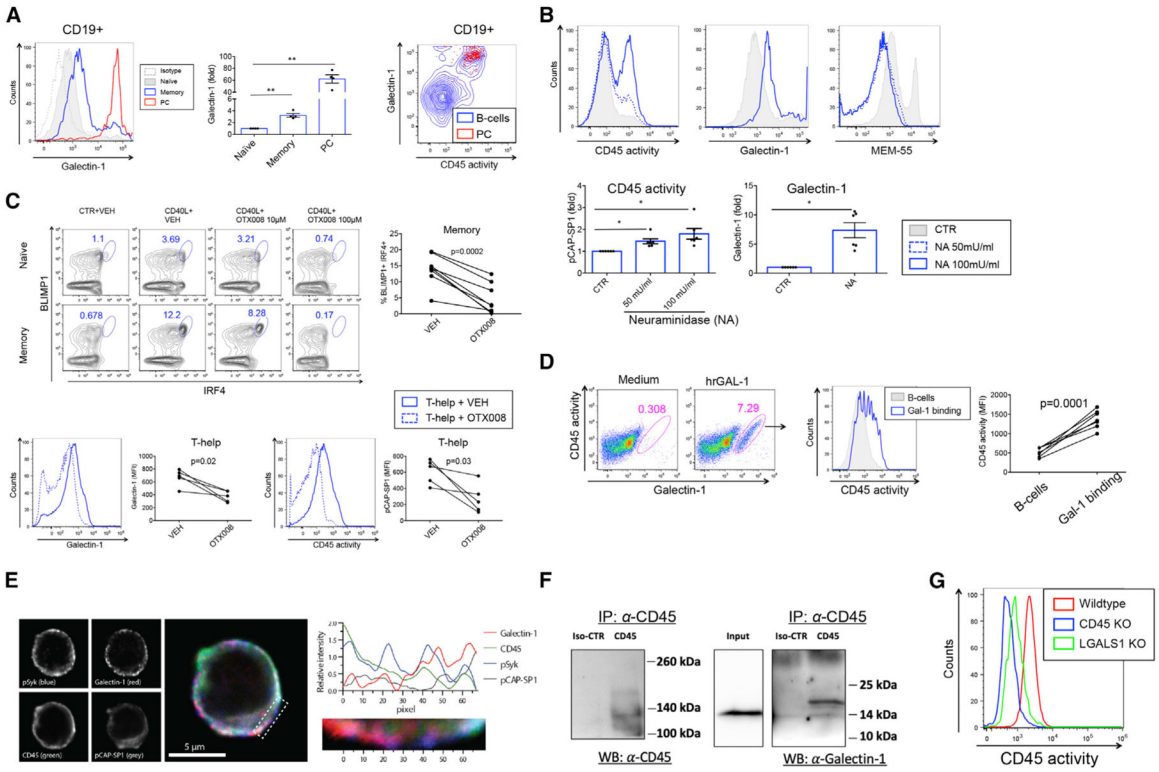

Figure 7. Galectin-1 enhances CD45 phosphatase activity and PC differentiation

(A) Flow cytometry histogram showing surface staining of Galectin-1 in naive (gray), memory (blue), and PCs (red) in human peripheral blood B cells (left panel). Isotype control is shown by gray-dotted histogram. Graph shows fold increase in surface Galectin-1 staining (MFI) relative to naive B cells (n = 4). Contour plot depicts CD45 activity versus Galectin-1 surface staining in B cells (blue) and PCs ($CD138^{hi}CD38^{hi}$) (red) backgated to CD45 $activity^{hi}Galectin\text{-}1^{hi}$ cells (right panel).

(B) Histograms show CD45 activity (left panel), Galectin-1 staining (middle panel), and MEM-55 staining (right panel) in CTR- or NA-treated B cells. Graphs show fold increase in MFI of CD45 phosphatase activity (left lower panel) and Galectin-1 staining (right lower panel) relative to CTR-treated B cells (n = 6).

(C) Upper panels: Dot plots show expression of IRF4 and BLIMP1 in naive B cells and MBCs differentiated toward ASCs in the presence of 10 and 100 μM OTX008 or VEH. Graph shows % $IRF4^{+}BLIMP1^{+}$ B cells in MBC cultures. Lower panels: Galectin-1 surface expression (left panel) and CD45 phosphatase activity (right panel) in VEH-treated (blue histogram) and OTX-treated (blue dotted histogram) MBCs. Graphs show MFI values of Galectin-1 staining (left) and CD45 activity (right) (n = 5).

(D) Flow cytometry dot plots show CD45 activity versus Galectin-1 surface staining in the presence of medium or rhGAL-1 (left panels). Histogram shows CD45 phosphatase activity of $Galectin\text{-}1^{hi}$ B cells with rhGAL1 (blue) and total B cells (gray) (middle panel). Graph shows MFI values of CD45 activity in total B cells (gray histogram) and $GAL\text{-}1^{hi}$ (blue open histogram) B cells (right panel) (n = 6).

(E) Representative localization of Galectin-1 relative to pSyk, pCAP-SP1, and CD45 in human B cells. The panels (left) present signals from the individual fluorescence detectors,

and the center image is a merge of all four channels. The graph (right) shows the average (z axis) fluorescence intensity for each (x axis) pixel number in the indicated area (below graph and dotted area on center figure).

(F) CoIP of CD45 of B cell lysates and immunoblotted with anti-CD45 (left) or anti-Galectin-1 (right).

(G) Flow cytometry histogram showing CD45 phosphatase activity in gated live Raji B cells with CRISPR-Cas9 knockdown of CD45 (blue), Galectin-1 (green), and wild-type (red). Related to Figures S7 and S8. *$p < 0.05$, **$p < 0.01$.

KEY RESOURCES TABLE

REAGENT or RESOURCE	SOURCE	IDENTIFIER
Antibodies		
PE-Vio770 Mouse monoclonal anti human CD45RO (clone UCHL1)	Miltenyi Biotec	Cat # 130–096-739; RRID:AB_2660972
FITC Mouse monoclonal anti human CD45RA (clone HI100)	BD PharMingen	Cat# 555488; RRID:AB_395879
PE Mouse monoclonal anti human CD45RB (clone MT4 (6B6))	BD PharMingen	Cat# 555904; RRID:AB_396215
Alexa Fluor 647 Mouse monoclonal anti human CD45RC (clone MT2)	BD PharMingen	Cat# 565857; RRID:AB_2869721
PE-Cy7 Mouse monoclonal anti human CD38 (clone HIT2)	BD PharMingen	Cat# 560677; RRID:AB_1727473
APC-H7 Mouse monoclonal anti human IgD (clone IA6–2)	BD PharMingen	Cat# 561305; RRID:AB_1727473
Alexa Fluor 700 Mouse monoclonal anti human CD27 (clone M-T271)	BD PharMingen	Cat # 560611; RRID:AB_1727454
APC-Vio770 Mouse monoclonal anti human CD138 (clone 44F9)	Miltenyi Biotec	Cat# 130–098-203; RRID:AB_2655042
PE Rat monoclonal anti human/mouse Blimp1 (clone 6D3)	BD PharMingen	Cat# 564702; RRID:AB_2738901
APC-Vio770 Mouse monoclonal anti human IgA (clone IS118E10)	Miltenyi Biotec	Cat# 130–107-052; RRID:AB_2659727
APC Mouse monoclonal anti human CD45RB (cloneMEM55)	Molecular Probes	Cat# A15702; RRID:AB_2534482
PE Mouse monoclonal anti human CD45RB (clone MEM55)	BioLegend	Cat# 310204; RRID:AB_314807
PerCP-Vio700 Mouse monoclonal anti human CD19 (clone LT19)	Miltenyi Biotec	Cat# 130–097-686; RRID:AB_2661299
PE Mouse monoclonal anti human IgD (clone IgD26)	Miltenyi Biotec	Cat # 130–094-539; RRID:AB_10828555
PE-Vio770 Mouse monoclonal anti human IgG (clone IS113B2.2.3)	Miltenyi Biotec	Cat# 130–107-054; RRID:AB_2661453
FITC Mouse monoclonal anti human CD27 (clone MT271)	Miltenyi Biotec	Cat# 130–093-184; RRID:AB_1036205
PE-Vio770 Mouse monoclonal anti human CD38 (clone IB6)	Miltenyi Biotec	Cat# 130–099-151; RRID:AB_2660384
APC Mouse monoclonal anti human IgM (clone SA-DA4)	Southern Biotech	Cat# 9020–11; RRID:AB_2687522
Alexa Fluor 700 Rat monoclonal anti-mouse/human B220 (clone RA3–6B2)	BioLegend	Cat # 103232; RRID:AB_493717
APC-Cy7 Rat monoclonal anti-mouse CD3 (clone 17A2)	BioLegend	Cat# 100222; RRID:AB_2242784
BV605 Rat monoclonal anti-mouse IgG1 (clone A85–1)	BD Horizon	Cat # 563285; RRID:AB_2738116
BV605 Rat monoclonal anti-mouse IgG2A/2B (clone R2–40)	BD PharMingen	Cat# 744294; RRID:AB_2742124
APC Mouse monoclonal anti human CD45 (clone 5B1)	Miltenyi Biotec	Cat# 130–091-230; RRID:AB_244233
PE-Cy7 Rat monoclonal anti mouse CD138 (clone 281–2)	BioLegend	Cat# 142514; RRID:AB_2562198
PerCP-Cy5.5 Rat monoclonal anti mouse/human GL7 antigen (clone GL7)	BioLegend	Cat# 144610; RRID:AB_2562979
Alexa Fluor 488 Rat monoclonal anti human/mouse IRF4 (clone IRF4.3E4)	BioLegend	Cat# 646406; RRID:AB_2563267
FITC Rat monoclonal anti-mouse CD38 (clone 90.4)	Miltenyi Biotec	Cat # 130–102-514; RRID:AB_2657875
Alexa Fluor 488 Mouse monoclonal anti human CD80 (clone 2D10)	BioLegend	Cat# 305214; RRID:AB_528873
BV605 Mouse monoclonal anti human CD273 (clone MIH18)	BD PharMingen	Cat# 742718; RRID:AB_2740996
BV711 Mouse monoclonal anti human IgG	BD PharMingen	Cat# 740796; RRID:AB_2740459
PO Mouse monoclonal anti human CD45 (clone HI30)	ThermoFisher	Cat# MHCD4530; RRID:AB_10376143
Alexa Fluor 647Mouse monoclonal anti human Galectin-1 (clone GAL1/1831)	Novus Biologicals	Cat# NBP2–54457AF647; N/A
PerCP-eFluor®710 Mouse monoclonal anti human/mouse Phospho-ERK1/2 (T202/Y204) (clone MILAN8R)	ThermoFisher	Cat# 46–9109-42; RRID:AB_2573872
PE Mouse monoclonal anti-pSyk (pTyr348) (clone I120–722)	BD Biosciences	Cat# 558529; RRID:AB_647247

REAGENT or RESOURCE	SOURCE	IDENTIFIER
PE Rabbit monoclonal anti-pSyk (Tyr525/526) (clone C87C1)	Cell Signaling	Cat# 6485S; RRID:AB_11220429
PE Monoclonal mouse anti human Ki67 (clone Ki-67)	BioLegend	Cat# 350504; RRID:AB_10660752
Mouse monoclonal anti human CD45 (clone F10–89-4)	Bio-Rad	Cat# MCA87GA; RRID:AB_324341
Mouse monoclonal IgG2A Negative Control	Bio-Rad	Cat# MCA929; RRID:AB_322268
Goat polyclonal anti human Galectin-1	R&D Systems	Cat# AF1152; RRID:AB_2136626
Polyclonal donkey anti-goat IgG HRP	R&D Systems	Cat# HAF109; RRID:AB_357236
Polyclonal goat anti-mouse IgG HRP	R&D Systems	Cat# HAF007; RRID:AB_357234
Mouse monoclonal anti human CD45 (clone HI30)	BioLegend	Cat# 304002; RRID:AB_314390
Mouse IgG1, k Isotype Ctr antibody	BioLegend	Cat# 400101; RRID:AB_2891079
Alexa Fluor 700 Rat monocloanla anti-mouse CD38 (clone 90)	ThermoFisher	Cat# 56–0381-82; RRID:AB_657740
APC-Vio770 Recombinant human anti B220(clone REA755)	Miltenyi Biotec	Cat# 130–110-849; RRID:AB_2658286
PerCP Mouse monoclonal anti human CD45 (clone 2D1)	BD Biosciences	Cat# 347464; RRID:AB_400307
APC-Cy7 Mouse monoclonal anti human CD45 (clone 2D1)	BD Biosciences	Cat# 348795; RRID:AB_400385
PE Mouse monoclonal anti human Galectin-1 (GAL1/1831)	Novus Biologicals	Cat# NBP-54457PE; N/A
BV711 Mouse monoclonal anti human IgG (clone G18–145)	BD PharMingen	Cat# 740796; RRID:AB_2740459
Alexa Fluor 700 Mouse monoclonal anti human IgD (clone IA6–2)	BioLegend	Cat# 348230; RRID:AB_2563335
PE-Cy7 Mouse monoclonal anti human CD38 (clone HIT2)	BD PharMingen	Cat# 560677; RRID:AB_1727473
APC-Vio770 Mouse monoclonal anti human CD138 (clone 44F9)	Miltenyi Biotec	Cat# 130–119-837; RRID:AB_2751876
PE Rat monoclonal anti mouse/human IRF4 (clone IRF4.3E4)	BioLegend	Cat# 646403; RRID:AB_2563004
CD27 Alexa Fluor 488 Mouse monoclonal anti human CD27 (clone QA17A18)	BioLegend	Cat# 393204, RRID:AB_2750089
Biotin Mouse monoclonal anti human PD-L2 (clone MIH18)	Miltenyi Biotec	Cat# 130–116-561; RRID:AB_2656873
PerCP-Vio700 Mouse monoclonal anti human CD19 (clone LT19)	Miltenyi Biotec	Cat# 130–113-171; RRID:AB_2725998
PE Mouse monoclonal anti human CD95 (clone DX2)	BioLegend	Cat # 305608; RRID:AB_314546
PE Mouse monoclonal anti human CD40 (clone 5C3)	BioLegend	Cat# 334308; RRID:AB_1186038
PE Mouse monoclonal anti human CXCR3 (clone G025H7)	BioLegend	Cat# 353706; RRID:AB_10962912
APC Mouse monoclonal anti-6x histidine (clone AD1.1.10)	Abcam	Cat# ab72579; RRID:AB_1267597)
PE Rat monoclonal anti mouse CD138 (clone 281–2)	BioLegend	Cat# 142504; RRID:AB_10916119
PE Rat monoclonal anti mouse GL7 (clone GL7)	BioLegend	Cat# 144608; RRID:AB_2562926
Goat polyclonal anti human Galectin-1 (purified goat IgG)	R&D Systems	Cat # AF1152; RRID:AB_2136626
Polyclonal goat IgG	R&D Systems	Cat # AB-108-C; RRID:AB_354267
Alexa Fluor 488 AffiniPure F(ab')2 Fragment Donkey Anti-Goat IgG(H+L)	Jackson ImmunoResearch	Cat# 705–546-147; RRID:AB_2340430
Goat F(ab')2 anti-human Lambda	Southern Biotech	Cat# 2072–01; RRID:AB_2795766
Goat F(ab')2 anti-human Kappa	Southern Biotech	Cat# 2062–01; RRID:AB_2795736
Alexa Fluor 488 Donkey anti-mouse	ThermoFisher	Cat# R37114; RRID:AB_2556542
Alexa Fluor 555 Donkey anti-goat	ThermoFisher	Cat# A21432; RRID:AB_2535853
Alkaline phosphatase conjugated goat anti-mouse IgG	Sigma-Aldrich	Cat# A2429; RRID:AB_258000
APC-Vio770 Mouse monoclonal anti human CD45 (clone 5B1)	Miltenyi Biotec	Cat# 130–096-609; RRID:AB_2660424
Biological samples		
Mouse tissue (LN, spleen, BM)	N/A	N/A
Human peripheral blood, BM	N/A	N/A

REAGENT or RESOURCE	SOURCE	IDENTIFIER
Chemicals, peptides, and recombinant proteins		
Mega CD40L (human recombinant)	Enzo Life sciences	Cat# ALX-522–110
Mega CD40L (murine recombinant)	Enzo Life sciences	Cat# ALX-522–120-C010
Recombinant Human IL-4	PeproTech	Cat# 200–04
Recombinant Human IL-21	PeproTech	Cat # 200–21
ODN2006	InvivoGen	Cat # tlrl-2006
PTP CD45 Inhibitor	Calbiochem	Cat# 540215
Fostamatinib (R406)	Selleckchem	Cat# S2194
OTX008 Calixarene 0118	Axon Medchem	Cat# Axon 2332
Pepinh-MYD (MyD88 Inhibitory Peptide)	InvivoGen	Cat# tlrl-pimyd
Recombinant human Galectin-1 protein	Novus Biologicals	Cat# NBP2–34878
Recombinant Mouse IL-4	PeproTech	Cat# 214–14
Recombinant Mouse IL-21	PeproTech	Cat# 210–21
Neuraminidase from *Vibrio Cholerae*	Sigma-Aldrich	Cat# N6514
Human TLR1–9 Agonist Kit tlrl-	InvivoGen	Cat# kit1hw
RPMI 1640 Medium, no phenol red	ThermoFisher	Cat# 11835030
Phosphatase substrate	Sigma-Aldrich	Cat# P4744
BS3 reagent	ThermoFisher	Cat# 21580
NuPAGE LDS sample buffer	ThermoFisher	Cat# NP0007
DTT	ThermoFisher	Cat# R0861
ProLong™ Gold Antifade Mountant	ThermoFisher	Cat# P10144
TRI reagent	Sigma Aldrich	Cat# T9424
Critical commercial assays		
Fixable Viability stain 510	BD PharMingen	Cat# 564406; RRID:AB_2869572
Taqman™ RNA-to-C_T™ 1-step Kit	ThermoFisher	Cat# 4392938
TaqMan™ gene expression assay *LGALS1 Hs00355202_m1*	ThermoFisher	Cat# 4331182
TaqMan™ gene expression assay *POLR2A Hs00172187_m1*	ThermoFisher	Cat# 4331182
TaqMan™ gene expression assay *PTPRC Hs04189704_m1*	ThermoFisher	Cat# 4331182
TaqMan™ gene expression assay *ERK Hs00385075_m1*	ThermoFisher	Cat# 4331182
TaqMan™ gene expression assay *SYK Hs00895377_m1*	ThermoFisher	Cat# 4331182
Human B Cell Nucleofector Kit	Lonza	Cat# VPA-1001
Silencer®Select siRNA PTPRC (s194730)	ThermoFisher Ambion	Cat# 4392420
Silencer Select Negative Control No. 1 siRNA	ThermoFisher Ambion	Cat# 4390843
HALT™ Protease and phosphatase inhibitor cocktail	ThermoFisher	Cat# 78441
Pierce™ IP Lysis Buffer	ThermoFisher	Cat# 87788
Transcription Factor Buffer Set	BD PharMingen	Cat# 562574
Dynabeads™ Protein G Immunoprecipitation Kit	ThermoFisher	Cat# 10007D
QIAGEN EndoFree Plasmid Maxi Kit	QIAGEN	Cat# 12362
Human IgM ELISA Kit	Invitrogen	Cat# 88–50620-22
Human IgG ELISA Kit	Invitrogen	Cat# 88–50550-88

REAGENT or RESOURCE	SOURCE	IDENTIFIER
Human TruStain FcX™	BioLegend	Cat# 422302
FcR Blocking Reagent human	Miltenyi Biotec	Cat# 130–059-901
Memory B cell Isolation Kit, human	Miltenyi Biotec	Cat# 130–093-546
Switched Memory B Cell Isolation Kit, human	Miltenyi Biotec	Cat# 130–093-617
CD138 MicroBeads, human	BD PharMingen	Cat# 130–051-301
Untouched™ B Cells	ThermoFisher	Cat# 11422D
Anti-Biotin MicroBeads	Miltenyi Biotec	Cat# 130–090-485
Experimental models: Cell lines		
Raji wt	ATCC	Cat# CCL-86; RRID:CVCL_0511
Raji Gal1 −/−	This paper	N/A
Raji CD45 −/−	This paper	N/A
Oligonucleotides		
hCD45: 5´-TGGCTTAAACTCTTGGCATT-3´,	This paper	N/A
hLGALS_s1: 5´-CGCCGTGGGCGTTGAAGCGA-3´	This paper	N/A
Recombinant DNA		
Cas9/gRNA vector pSpCas9(BB)-2A-GFP (PX458)	Dr. Feng Zhang Addgene repository; Addgene #48138	N/A
anti–MHC II–HA	Grodeland et al., 2013	N/A
Software and algorithms		
FlowJo (Treestar)	FlowJo, LLC	https://www.flowjo.com/
Prism	GraphPad	http://www.graphpad.com/scientific-software/prism
ImageJ	National Institutes of Health	https://imagej.nih.gov/ij/
Other		
Superfrost Plus microscopy slides	Thermo Fischer	Cat# 10149870
Shandon™ Double Cytofunnel™	Thermo Fischer	Cat# 12016679